CHAPTER 1: INTRODUCTION

Despite cervical cancer having a good prognosis through early detection, it is the second most common cancer and cancer-related mortality in women worldwide with an estimated 529,409 new cases and 274,883 deaths in 2008 (WHO/ICO Information Centre on HPV and Cervical Cancer, 2010). Incidence and mortality rates in developed countries were lower due to effective cervical screening and on-going active health education programs as compared to developing countries, which accounts for 86% of cervical cancer cases worldwide (Parkin *et al*., 2001). In Malaysia, a total of 1,074 cases of cervical cancer were registered by National Cancer Registry (NCR) in 2006, making it the third most common cancer in women after breast and colorectal cancer (Zainal *et al*., 2006).

Cisplatin (CDDP) is a platinum-based anti-cancer drug widely-used in treatment of various cancers such as ovarian, testicular, lung, cervical as well as head and neck carcinomas (Page and Takimoto, 2004). While treatment usually results in initial partial responses and disease stabilization, its long-term success is hindered by dose-limiting toxicities and the development of drug resistance (Szakas *et al*., 2006). Despite extensive development of cisplatin analogues, only very few have entered clinical trials, with the resulting approved drugs such as carboplatin and oxaliplatin having limited advantages over cisplatin (Wong and Giandomenico, 1999). Combination therapies with multiple drugs or with multiple modalities have been introduced over the years in the treatment of cancers to improve therapeutic efficacy through a synergistic drug interaction. The use of combination therapies were found to be superior compared to mono-targeted therapies as it induces maximum cell kill and is applicable to a broader spectrum of heterogeneous tumor cells resistant to a specific drug. Furthermore, this

multi-targeted approach can also decelerate the development of drug resistant sub-clones of tumor cells (Zoli *et al*., 2001).

Natural bioactive compounds have been extensively used in the treatment of cancer for many years either as standalone or as adjuvants to improve therapeutic efficacy by reducing drug-induced toxicity and drug resistance (Mahendele *et al*., 2005; Wang *et al*., 2005). One example is the naturally occurring phenylpropanoid, 1'S-1'-acetoxychavicol acetate (ACA) isolated from the wild ginger, *Alpinia conchigera* Griff. ACA has been shown to exhibit various biological activities in previous studies such as the inhibition of tumor promoter-induced Epstein-Barr virus activation (Kondo *et al*., 1993), and the induction of apoptosis in Ehrlich ascites tumor cells through modulation of polyamine metabolism and caspase-3 activation (Moffatt *et al*., 2005). Furthermore, ACA was shown to inhibit the cellular growth of myeloid leukemic cells *in vitro* and *in vivo* through induction of apoptosis via mitochondrial- and Fas-mediated dual mechanism (Ito *et al*., 2004). More recently, it was reported that ACA induced comparable levels of dose- and time-dependent cytotoxicity on a variety of other tumor cell lines to current commercial anti-cancer drugs, without any adverse effects on normal cells (Khalijah *et al*., 2010).

MicroRNAs (miRNAs) are a class of evolutionary conserved small non-coding RNAs that regulate target genes post-transcriptionally (Bartel, 2004). MiRNAs are found in abundance in many human cell types (Lim *et al*., 2003) and are thought to regulate the expression of around 60% of mammalian genes (Friedman *et al*., 2009), making them one of the largest classes of gene regulators. It was postulated that a single miRNA is capable of regulating up to 100 different target mRNAs (Lim *et al*., 2005; Brennecke *et al*., 2005), and that each of these miRNAs play critical roles in various

biological processes such as human tumorigenesis (Michael *et al*., 2003), cell proliferation and metabolism (Brennecke et al., 2003), and programmed cell death (Baehrecke, 2003). As many of these biological processes are pertinent to chemosensitivity and chemoresistance, it is hypothesized that miRNAs could play an important role in modulating responses toward anti-cancer drugs.

In this study, the combined effects of ACA and CDDP on human cervical carcinoma cells Ca Ski were investigated to determine the ability of ACA in potentiating the effects of CDDP, a platinum-based anti-cancer drug widely-used in treatment of various cancers, including cervical cancer. The responsive miRNAs towards these drugs were also determined to identify miRNAs that might be involved in response towards ACA and/or CDDP. *In silico* determination of gene targets corresponding to selected candidate miRNAs were also identified and a hypothetical pathway model involving miRNAs interaction with their gene targets was proposed to elucidate the possible mechanism of miRNAs in regulating anti-cancer drug response.

1.1 Study objectives

The main objectives for this study were:

i. To investigate the cytotoxic effects of ACA and CDDP on human cervical carcinoma cells Ca Ski.

ii. To evaluate the combined effects of ACA and CDDP on human cervical carcinoma cells Ca Ski.

iii. To identify the changes in global miRNA expression patterns upon administration of ACA and/or CDDP on human cervical carcinoma cells Ca Ski.

iv. To propose a hypothetical pathway model comprising of miRNAs interaction with their putative target genes involved in response towards ACA and/or CDDP.

CHAPTER 2: LITERATURE REVIEW

2.1 Cancer

2.1.1 Overview

According to the National Cancer Institute (NCI), cancer is a group of diseases where abnormal cells divide without control and become capable of invading other tissues. These abnormal cells arise from a group of cells which are no longer subjected to normal cellular growth control to form a mass of tissue known as a tumor (National Cancer Institute, 2010a). The comparison between cell division in normal cells and cancer cells are shown in Figure 2.1.

Tumors can either be benign or malignant. Benign tumors are not cancerous and they do not spread to other parts of the body while malignant tumors are cancerous cells capable of invading nearby tissues and spreading to other parts of the body in a process known as metastasis (National Cancer Institute, 2010a). Approximately 90% of human cancer deaths are thought to be caused by metastases (Sporn, 1996). Nevertheless, some cancers do not form tumors and one example is leukemia, cancer of the bone marrow and blood.

Cancer can either be caused by external factors such as chemical, radiation and infectious organisms or internal factors such as inherited mutations, hormones and immune conditions. These factors often act together or in sequence to initiate or promote carcinogenesis and in most cases, cancer is only detected after ten or more years from the time of exposure to external factors. The standard treatments in cancer currently are surgery, chemotherapy, radiation, hormonal therapy, biological therapy and targeted therapy (American Cancer Society, 2010a).

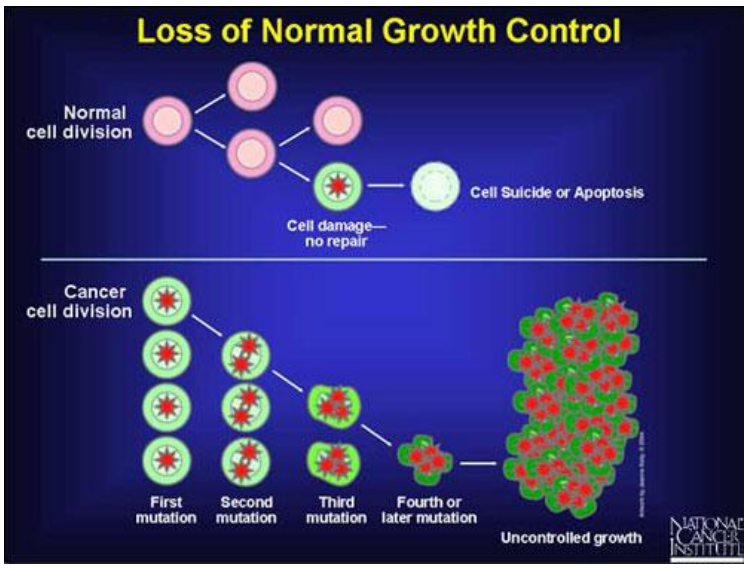

Figure 2.1: Comparison between cell division in normal cells and cancer cells (figure adapted from National Cancer Institute, 2010a)

2.1.2 Multistep carcinogenesis

Carcinogenesis is the process in which normal cells are transformed into cancer cells. It is a prolonged multistep process in which a single cell of origin acquires a series of stable genetic mutations that allows for its sequential selection (Nowell, 1976). These susceptible cells gain a selective growth advantage and undergo clonal expansion as a result of activation of proto-oncogenes and/or inactivation of tumor suppressor genes and/or altered expression of cancer-associated molecules due to genetic or epigenetic damage (Fearon and Vogelstein, 1990; Harris, 1991; Knudson, 1986). Studies have found that multiple rate-limiting steps are involved in tumorigenesis in mice (Bergers *et al*., 1998). Furthermore, human cells have been found to be harder to transform compared to rodent cells even though the rodent cells require at least two introduced genetic changes before they acquire tumorigenic competence (Hahn *et al*., 1999). These findings further strengthen the belief that carcinogenesis is a multistep process. Nevertheless, studies have found that carcinogenesis can be divided into three distinct

stages: initiation, promotion and progression (Hennings *et al*., 1993) and this multistep carcinogenesis is depicted in Figure 2.2.

Initiation is the first stage of carcinogenesis which is an irreversible process involving mutations in the DNA. These mutations are usually single base mutations and are often caused by genotoxic carcinogens such as chemicals, radiation or virus resulting in activation of proto-oncogene and/or inactivation of tumor suppressor genes (Bishop, 1991; Marshall, 1991). Promotion is the second stage following initiation leading to the formation of pre-neoplastic lesion. The latent phenotype of the initiated cell is expressed through cellular selection and clonal expansion by increasing cell proliferation and/or inhibition of cell death, which is caused by toxicity, terminal differentiation or mito-inhibition of the non-initiated cells and mitogenesis of the initiated cells (DiGiovanni, 1992). As this stage occurs over a long period of time and requires the continued presence of tumor promoters, it is reversible in the early stages. Progression is the final and irreversible stage which results in conversion of benign tumors into malignant neoplasms capable of invading nearby tissues and metastasizing to distant sites in the body due to repetitive mutations and epigenetic changes (DiGiovanni, 1992).

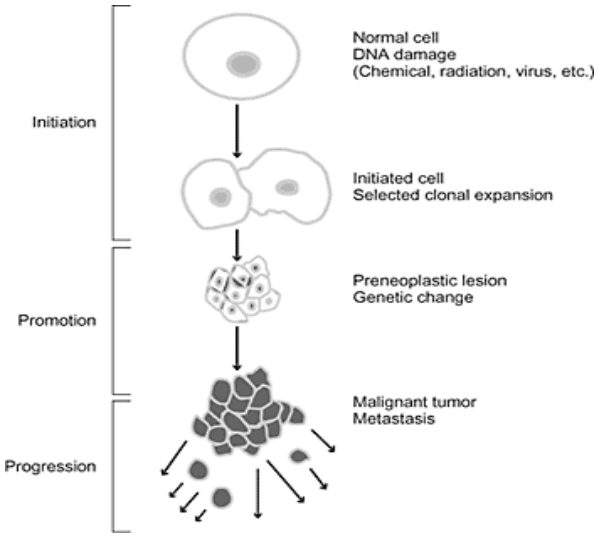

Figure 2.2: Multistep carcinogenesis (figure adapted from Cortés-Funes, 2002)

2.2 Cervical cancer

2.2.1 Overview

Cervical cancer is defined as the formation of cancer in the tissues of cervix by the NCI (National Cancer Institute, 2010b). It is usually a slow-growing cancer that may not display any symptoms initially, but can be detected with cytology-based screening using Papanicolaou (Pap) smear tests, where some cells are scraped from the cervix and viewed under the microscope. The cervix is the lower part of the uterus (womb) that connects the uterus and vagina. The upper part of the cervix that is closer to the uterus is called the endocervix while the lower part of the cervix that is closer to the vagina is called the exocervix (or ectocervix). Most cervical cancers begin in the transformation zone, where the two parts of the cervix meet because these cells in the transformation zone are less stable and thus more susceptible to viral infections (American Cancer Society, 2010b).

2.2.2 Cervical cancer subtypes

There are several biological types of primary cervical neoplasm. Nearly 80 to 90% of cervical cancers are squamous cell carcinomas which arise from the squamous cells that cover the surface of the exocervix. Squamous cell carcinomas often begin where the exocervix joins the endocervix. Although only 10 to 20% of cervical cancers are adenocarcinomas which develop from the mucus-producing gland cells of the endocervix, it is getting more common in women born in the last 20 to 30 years. Besides squamous cell carcinomas and adenocarcinomas, cervical cancers that share the characteristics of both types of cancers known as adenosquamous carcinomas or mixed carcinomas can also arise, although it is less common (American Cancer Society, 2010b).

2.2.3 Etiology of cervical cancer

Even though the main causal factor for cervical cancers is the human papillomavirus (HPV), cervical cancer is a multi-factorial disease like any other cancer which can be caused by various other factors such as environmental co-factors and genetic factors. This was evidenced in epidemiological studies which showed that HPV infection itself is often not sufficient to cause neoplasia in cervix as its infection is limited and can be resolved by itself. Therefore, only a small fraction of women with HPV infection will progress to cervical cancer although most women would be infected with HPV at least once in their lifetime (Franco *et al*., 1999; Ho *et al*., 1998).

The link between sexually transmitted HPV and cervical cancers was discovered by zur Hausen *et al*., in 1981. High-risk HPVs such as HPV16, HPV18 and HPV31 have been detected in up to 99.7% of cervical squamous cell carcinomas and 94 to 100% of cervical adeno- and adenosquamous carcinomas (Walboomers *et al*., 1999; Castellsague *et al*., 2006). The oncoproteins E6 and E7 produced by the high-risk HPVs contribute to cervical cancer by inactivating the cellular tumor suppressor proteins p53 and pRb, respectively (Scheffner *et al*., 1990; Dyson *et al*., 1989; Boyer *et al*., 1996).

The investigation which was carried out by the International Agency for Research on Cancer (IARC) on the possible roles of environmental co-factors in more than 2,000 cases of invasive cervical carcinoma showed that the HPV DNA was identified in only 24% of the cases but HPV DNA plus one of the environmental co-factors was identified in 75% of the cases. These co-factors possibly interact with the genetic factors to adjust the nature of HPV infection (Bosch and Muñoz, 2002). Among some examples of the environment co-factors which could play a role in cervical cancers are tobacco smoking (Deacon *et al*., 2000; Hildesheim *et al*., 2001), sexually

transmitted disease such as *Herpes simplex virus*-2 (HSV-2) (Smith *et al*., 2002a) and *Chlamydia trachomatis* (*C. trachomatis*) (Smith *et al*., 2002b) as well as diet and nutrition (García-Colsas *et al*., 2005).

2.2.4 Cervical carcinogenesis

Cervical cancers are thought to arise from a cervical lesion which is caused by the long persistent infection of high-risk HPV (zur Hausen, 2002). Studies have also shown that low levels of E6 and E7 expression are often found in mild and moderate dysplasia lesions whereas severe dysplasia and invasive carcinoma displayed high level of E6 and E7 expression (Klaes *et al*., 1999), indicating that persistent infection of oncogenic HPVs is necessary for progression and invasion in cervical cancer. The major steps in cervical carcinogenesis have been elucidated by Schiffman and Kjaer (2003) and are depicted in Figure 2.3. Cervical carcinogensis was found to consist of HPV infection of normal cervix (offset by HPV clearance), persistent infection with HPV over a long period, progression of HPV-infected cervix to pre-cancer (partly offset by regression of pre-cancer) and invasion. The HPV-infected cervix is often but not necessarily associated with mild cytologic and/or histologic abnormalities.

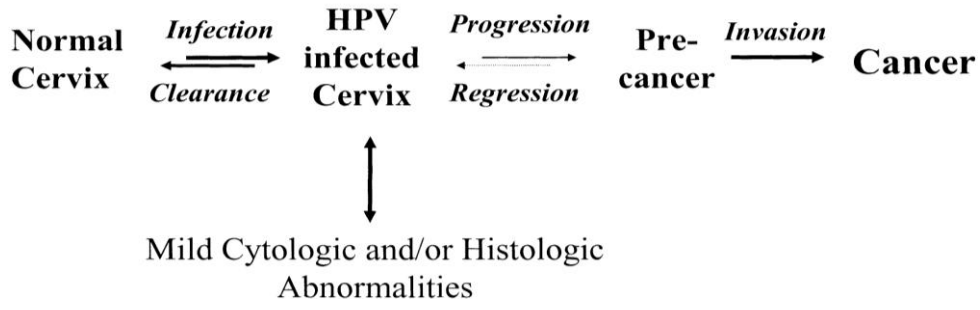

Figure 2.3: Cervical carcinogenesis (figure adapted from Schiffman and Kjaer, 2003)

2.2.5 Grading in cervical cancer

Just like any other cancer, cervical cancer is the result of a multistep process that involves the transformation of the normal cervical epithelium to a pre-neoplastic cervical intraepithelial neoplasia that is subsequently transformed into invasive cervical cancer (DiSaia *et al*., 2002; Richart, 1990). A disturbed proliferation of squamous cells is called dysplasia or cervical intraepithelial neoplasia (CIN) and is the precursor of invasive carcinoma. The CIN grading is based on the severity and proportion of the epithelial layer with neoplastic changes where in CIN I a third, in CIN II two third and in CIN III (almost) the total layer of epithelium contains atypical cells. The likelihood of progression of CIN I, CIN II and CIN III to invasive carcinoma ranges from 0.4 to 1%, 1.2 to 5% and 3.9 to greater than 12%, respectively (Holowaty *et al*, 1999; Nasiell *et al*., 1986; Ostör, 1993).

2.2.6 Staging of cervical cancer

The different clinical stages of invasive cervical cancer are defined by the Fédération of Internationale de Gynécologic et d'Obstétrique (FIGO) and consist of four broad stages with sub-stages within each stage for better classification. The four broad stages are Stage I, II, III and IV. Stage I is carcinoma that is strictly confined to the cervix, Stage II is carcinoma that extends beyond the cervix, but does not extend into pelvic wall (involves the vagina but not as far as the lower third of vagina), Stage III is carcinoma that extended to pelvic wall and lower third of the vagina while Stage IV is carcinoma that extended beyond pelvis and involves the mucosa of bladder and/or rectum (FIGO, 1971; Creasman, 1995; Shepherd, 1996).

Table 2.1: FIGO staging of cervical carcinomas

Stage I – Limited to the cervix **IA** - diagnosed only by microscopy, no obvious lesion • IA1 – stromal invasion < 3mm depth and ≤ 7mm spread • IA2 – stromal invasion 3-5mm depth and ≤ 7 mm spread **IB** – visible lesion with invasion > 5 mm depth or > 7mm spread • IB1 – lesion ≤ 4cm in dimension • IB2 – lesion > 4 cm dimension
Stage II – Invades beyond cervix but does not extend into pelvic wall (involves the vagina but not as far as the lower third of vagina) **IIA** – without parametrial invasion but involve up to upper two-third of vagina **IIB** – with parametrial invasion
Stage III – extends to pelvic wall/lower one-third of vagina **IIIA** – involves lower one-third of vagina **IIIB** – extends to pelvic wall and/or causes hydronephrosis or non-functioning kidney
Stage IV– extends beyond pelvis and involves the mucosa of bladder and/or rectum **IVA** – spread into adjacent pelvic organs **IVB** – spread to distant organs

2.2.7 Epidemiology in cervical cancer

Although cervical cancer is one of the few cancers that can be prevented since the pre-cancerous cells can be detected in the early stage by screening, studies have found that cervical cancer is one of the leading causes of cancer-related deaths among women worldwide, especially in developing countries. It is estimated that one in ten female cancers diagnosed worldwide is cervical cancer, making it the second most common cancer in women worldwide. (Ferlay *et al*., 2004). It is also estimated that there are more than 273 000 deaths from cervical cancer worldwide each year which accounts for 9% of female cancer deaths. More than 2.7 million years of life are lost among women between the ages of 25 to 64 worldwide with some 2.4 million in developing countries and only 0.3 million in developed countries (Yang *et al*., 2004). The numbers of incidences in developed countries are lower due to the availability of cervical screening and on-going active health education programs (Parkin *et al*., 2001).

In Peninsular Malaysia, cervical cancer is the third most common cancer in women after breast cancer and colorectal cancer with Chinese women having the highest incidence followed by the Indians and Malays in a comparison between major races. A total of 1,074 cases were registered with National Cancer Registry (NCR) in 2006 and the overall age-standardized incidence rate (ASR) was 12.2 per 100,000 population. Study conducted by the NCR found that the incidence rate increased with age after 30 years old and peaks at 60-69 years old (Zainal *et al*., 2006).

2.2.8 Human epidermoid cervical carcinoma Ca Ski

The human cervical carcinoma cells Ca Ski which was derived from the metastatic site in the small bowel mesentery of 40 years old female Caucasian was used in this study. It is a hypotriploid, adherent cell line with epithelial-like morphology as well as having cellular products of beta subunit of human chorionic gonadotropin (hCG) and tumor associated antigen (Pattillo *et al*., 1977). In addition, these cells have also been reported to contain an integrated HPV-16 genome (about 600 copies per cell) and sequences related to HPV-18 (Yee *et al*., 1985).

2.3 Cell cycle

2.3.1 Overview

Cell division consists of two consecutive processes which can be divided into two stages: mitosis and interphase. Mitosis (M) phase consists of prophase, metaphase, anaphase and telophase while interphase consists of G_1, S and G_2 phases. DNA replication occurs in S phase, which is after G_1 phase (in which cells prepares for DNA synthesis), and before G_2 phase (in which cells prepare for mitosis). Thus, the cell cycle is often subdivided into G_1, S, G_2 and M phases although cells in G_1 phase can also enter a resting state know as G_0 phase under unfavorable conditions. Cells in G_0 phase does not undergo senescence but remain non-growing and non-proliferating, and can re-enter the cell cycle when conditions become favorable. The progress of cells from one phase to another is tightly regulated by various regulatory proteins.

2.3.2 Cell cycle regulation

Among key regulatory proteins involved in cell cycle regulation are cyclin-dependent kinases (CDK) and cyclin proteins. CDKs are serine/threonine protein kinases which are activated at specific points in cell cycle and five such CDKs have been identified to be active in different phases: G_1 phase (CDK4, CDK6 and CDK2); S phase (CDK2); G_2 and M phase (CDK1). In contrast to CDKs whose protein levels remain stable throughout the cell cycle, cyclin protein levels changes during the cell cycle and in doing so, activate CDK sporadically as different cyclin-CDK complex is required at different phases (Evans *et al*., 1983; Pines, 1991). The three types of cyclin D (cyclin D1, cyclin D2 and cyclin D3) synthesis are stimulated by growth factors, unlike other cyclin proteins (Assoian and Zhu, 1997). Cyclin D forms a complex with CDK4 or CDK6 and these cyclin D-CDK4/6 complexes are required for G_1 phase progression (Sherr, 1994) while cyclin E binds with CDK2 to regulate progression from

G_1 to S phase (Ohtsubo *et al*., 1995). On the other hand, cyclin A is required in both S and G_2 phase by forming a complex with CDK2 in S phase and complexes with CDK1 in G_2 phase to promote entry into M phase (Girard *et al*., 1991; Walker and Maller, 1991). Progression into M phase is also regulated by cyclin B-CDK1 complex (King *et al*., 1994; Arellano and Moreno, 1997). A summary of cell cycle regulation is depicted in Figure 2.4.

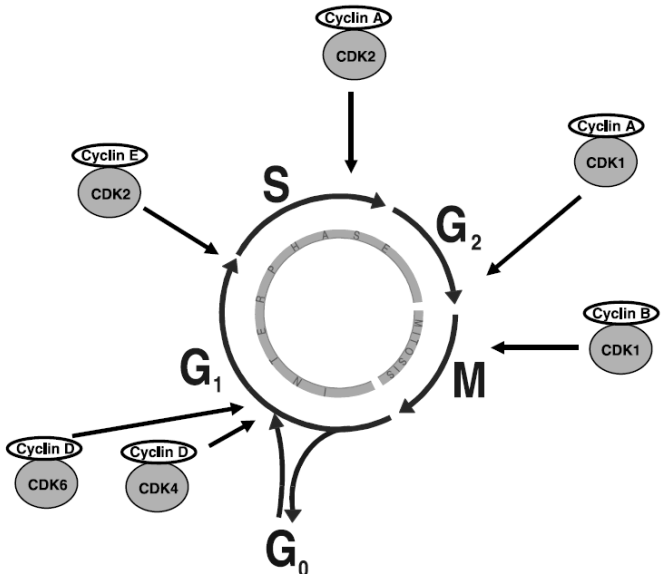

Figure 2.4: Cell cycle regulation (figure adapted from Vermuelen *et al*., 2003)

Besides these CDK and cyclin proteins, there are also cell cycle inhibitory proteins which regulate CDK activity known as CDK inhibitors (CKI). These CKI proteins consist of two distinct families, the INK4 family and Cip/Kip family (Sherr and Roberts, 1995) and are summarized in Table 2.2. The INK4 family consisting of p15 (INK4b), p16 (INK4a), p18 (INK4c) and p19 (INK4d) inactivate G_1 CDK (CDK4 and CDK6) by forming stable complexes and preventing their association with cyclin D (Carnero and Hannon, 1998). The Cip/Kip family on the other hand consists of p21 (Waf1, Cip1), p27 (Cip2) and p57 (Kip2) and they inhibit G_1 CDK-cyclin complexes, and to a lesser extent, CDK1-cyclin B complexes (Polyak *et al*., 1994; Harper *et al*., 1995; Lee *et al*., 1995; Hengst and Reed, 1998). These CKI proteins are regulated by

both internal and external stimuli: p21 is activated by p53 tumor suppressor gene (el-Deiry *et al*., 1993) while p15 and p27 are activated by transforming growth factor-β (TGF-β) (Reynisdóttir *et al*., 1995).

Table 2.2: Cyclin-dependent kinase inhibitor (CKI) proteins (adapted from Vermuelen *et al*., 2003)

CKI family	Function	Family members	
INK4 family	Inactivation of G_1 CDK (CDK4, CDK6)	p15	(INK4b)
		p16	(INK4a)
		p18	(INK4c)
		p19	(INK4d)
Cip/Kip family	Inactivation of G_1 cyclin-CDK complexes and cyclin B-CDK1	p21	(Waf1, Cip1)
		p27	(Cip2)
		p57	(Kip2)

Besides these regulatory proteins, there are also restriction point and checkpoints to ensure orderly progression in cell cycle. The restriction point (R) is found in G_1 phase, whereby cells that passed through this point are committed to enter the cell cycle (Pardee 1974). The other checkpoints which can arrest the cell cycle to allow for DNA repair are the G_1-S checkpoint (before cells enter S phase) and G_2-M checkpoint (after DNA replication). Cell cycle arrest at G_1-S checkpoint is induced by p53 through transcription of several genes such as *p21* and *Bax* (Agarwal *et al*., 1998). The p21 is a CKI protein which inhibits CDK, resulting in cell cycle arrest to prevent replication of damaged DNA and allow for the damaged DNA to be repaired (Ko and Prives, 1996). However, if the DNA is severely damaged and beyond repair, p53 would then induce cell death through activation of genes involved in apoptotic signaling (Polyak *et al*., 1997). On the other hand, G_2-M checkpoint can be induced in absence of p53 through protein kinases Chk1 and Chk2, which are activated by ataxia-telangiectasia-mutated (ATM). Phosphorylation of Cdc25 by Chk1 and Chk2 promotes its binding to 14-3-3

proteins and sequestered it from nucleus, hence prevents it from activating CDK1-cyclin B complex (Sanchez *et al*., 1997; Zeng *et al*., 1998). Similar to G_1-S checkpoint, p53 can also induced the transcription of *p21* in G_2-M checkpoint, as well as *14-3-3 sigma* (*14-3-3* σ) which binds to cyclin B, resulting in cell cycle arrest (Taylor and Stark, 2001).

2.3.3 Cell cycle and cancer

In cancer, mutations can occur in genes involved in cell cycle such as CDKs, cyclins, and CKIs, resulting in uncontrolled cell proliferation. Alterations in expression of CDKs have been reported in cancer, although with low frequency. For example, CDK4 overexpression has been reported in various cell lines, melanoma, sarcoma and glioma as a result of amplification (Wolfel *et al*., 1995), as well as overexpression of CDK1 and CDK2 in colon adenomas and focal carcinomas in ademotous tissues (Yamamoto *et al*., 1998; Kim *et al*., 1999). Gene mutations which resulted in loss of binding sites for CKIs such as those found in *CDK4* and *CDK6* have also been identified in neuroblastoma (Easton *et al*., 1998).

Besides CDKs, deregulation in cyclins expression has also been linked to many cancers. Amplification in cyclin D1 have been reported in breast, esophageal, bladder, lung and squamous cell carcinomas (Hall and Peters, 1996), while overexpression and/or amplification of *cyclin D2,* and *cyclin E* are also reported in several cancers such as breast and colorectal cancer (Leach *et al*., 1993; Keyomarsi *et al*., 1995). Both cyclin A and cyclin E are also found to be overexpressed in lung carcinoma, whereby overexpression of cyclin A correlated with shorter survival (Dobashi *et al*., 1998).

Perturbations in expression of CKI proteins which inhibits cell cycle progression are also found in a wide range of cancers. Inactivation of *p16* can occur through deletions, point mutations or hypermethylations (Kamb, 1998) and inactivation of this gene have been reported in 50% of gliomas and mesotheliomas, 40 to 60% of nasopharyngeal, pancreatic and bilary tract tumors as well as 20 to 30% acute lymphoblastic leukemias (Hall and Peters, 1996). As *p16* and *p19* share the same locus (ARF-INK4), large deletions in this locus can also affect the expression of *p19,* while *p15* is also often deleted together as well since it is located near to *p16* (Harper and Elledge, 1996). Studies have also found that the loss of *p27* expression in many cancers correlated with poor prognosis and increased tumor aggressiveness (Philipp-Staheli *et al*., 2001; Slingerland and Pagano, 2000). Alterations in expression of p18 and p21 have also been reported in breast and thyroid cancer, respectively (Lapointe *et al*., 1996; Shi *et al*., 1996).

2.4 Cell death

2.4.1 Overview

The two major modes of cell death are apoptosis and necrosis. Apoptosis, also known as programmed cell death, is a controlled, energy-dependent cell death that does not results in inflammation as opposed to necrosis, an uncontrolled, energy-dependent cell death resulting in inflammation to neighboring cells (Elmore, 2007). Hence, apoptosis is the preferred mechanism in killing cancer cells in chemotherapy.

2.4.2 Apoptosis

The morphological hallmarks of apoptosis are cell shrinkage, chromatin condensation, cytoplasmic blebbing as well as formation of apoptotic bodies which are engulfed by macrophages and parenchymal cells (Kerr *et al*., 1972). On the other hand, nuclear fragmentation (DNA degradation by DNAses that cut the internucleosomal regions into double-stranded DNA fragments of 180-200 bp) is a well-known biochemical hallmark of apoptosis (Wyllie, 1980).

To date, there are three apoptotic pathways which have been identified: the extrinsic or death-receptor pathway, the intrinsic or mitochondrial pathway and the perforin/granzyme pathway. These pathways are depicted in Figure 2.5. Although these pathways are initiated differently, they converge on the same execution pathway involving caspase-3, an executioner caspase which plays an important role in triggering caspase cascade that eventually leads to apoptosis.

The death receptors, which are members of tumor necrosis factor (TNF) receptor gene superfamily, are involved in activating apoptosis in extrinsic pathway (Locksley *et al*., 2001). These members share a similar cysteine-rich extracellular domains as well as

a cytoplasmic domain of about 80 amino acids known as “death domains” which play a critical role in transmitting death signal from outside the cell to activate the extrinsic pathway (Ashkenazi and Dixit, 1998). The binding of Fas ligand to Fas receptor results in binding of adaptor protein FADD while the binding of TNF ligand to TNF receptor results in binding of adaptor protein TRADD which will then recruit FADD and RIP. FADD would then form the death-inducing signaling complex (DISC) together with procaspase-8, resulting in auto-catalytic activation of procaspase-8 which then activates the execution pathway involving caspase-3 (Kischkel *et al*., 1995).

On the other hand, the intrinsic pathway is activated by intracellular signals that may act positively (radiation, toxins, hypoxia, viral infections and free radicals) or negatively (absence of growth factors, cytokines and hormones) (Elmore, 2007). These stimuli would lead to changes in mitochondrial permeability transition (MPT), resulting in loss of mitochondrial membrane potential and leads to release of cytochrome c, an electron transport chain protein. The cytochrome c would then accumulate in the cytoplasm and binds with Apaf-1 and procaspase-9 to form apoptosome (Garrido *et al*., 2006). This complex then activates procaspase-9 into caspase-9, leading to activation of the execution pathway (Kaufmann and Hengartner, 2001).

The perforin/granzyme pathway is utilized by cytotoxic T-cells in mediating cytotoxicity. This apoptosis pathway is activated by the transmembrane pore-forming molecule perforin, with a subsequent exophytic release of cytoplasmic granules containing granzyme A or granzyme B through the pore and into the target cell (Trapani and Smyth, 2002). The granzyme A pathway activates caspase-independent cell death by via single-stranded DNA damage (Martinvalet *et al*., 2005) while granzyme B activates the mitochondrial pathway (Goping *et al*., 2005).

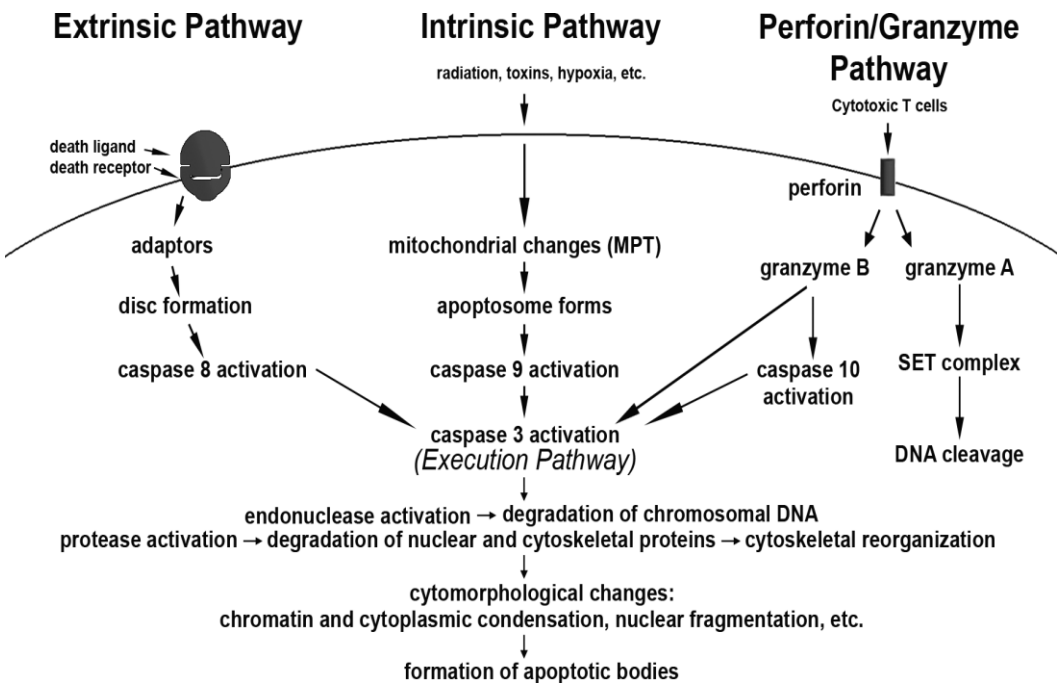

Figure 2.5: Apoptotic pathways (figure adapted from Elmore, 2007)

2.4.3 Apoptosis and cancer

The capability of cancer cells to increase their population numbers depends on not only the rate of cell proliferation, but also the rate of cell attrition. Apoptosis represents the major source of cell attrition, especially the extrinsic and intrinsic apoptotic pathways. Mutations in these pathways resulting in resistance towards apoptosis have been identified as a major hallmark in many, if not all types of cancer (Hanahan and Weinberg, 2011).

It was in 1972 that the possibility of apoptosis serving as a barrier to cancer was first raised, when it was reported that wide-spread apoptosis occurred in fast-growing and hormone-dependent tumor cells following hormone withdrawal (Kerr *et al*., 1972). The discovery of the anti-apoptotic activity of the *Bcl-2* oncogene (Vaux *et al*., 1998) led to the start of many investigations of apoptosis in cancer at the molecular level. Since then, various functional studies conducted have further reinforced the consensus

that apoptosis served as a barrier to cancer (Evan and Littlewood, 1998; Lowe *et al*, 2004).

In order for cancer cells to proliferate infinitely and increase their population numbers, they must evade apoptosis. Cancer cells acquire resistance to apoptosis through a variety of strategies and one of these is mutation in the *p53* tumor suppressor gene. Inactivation of p53 protein, a key component in DNA damage sensing that can induce the apoptotic pathway, has been reported in 50% of cancers in humans (Harris, 1996). Besides this, extracellular factors such as IGF-1/2 and IL-3, intracellular signals from Ras, and loss of pTEN expression can confer survival signals and activate PI3K-AKT pathway, which transmits anti-apoptotic signals and allows cancer cells to evade apoptosis (Evan and Littlewood, 1998; Downward, 1998; Cantley and Neel, 1999). It was also reported that Fas-death signaling is abrogated in a high proportion of lung and colon carcinoma cells (Pitti *et al*., 1998).

The elucidation of signaling circuitry governing apoptosis has revealed how apoptosis is triggered in response to various physiologic stresses in cells and this apoptotic circuitry is often attenuated at some point in tumors, enabling them to progress to high-grade malignancy (Adams and Cory, 2007; Lowe *et al*., 2004). The understanding of this circuitry has allowed for it to be exploited in cancer treatments which are aimed at restoring the defective apoptotic programs found in cancer cells or by inducing apoptosis through manipulation in the expression of genes involved in apoptosis regulation.

2.5 Chemotherapy

2.5.1 Overview

Chemotherapy is one of the commonly used treatments in cancers besides surgery and radiation and refers to the use of drugs to kill cancer cells (National Cancer Institute, 2010c). Unlike surgery and radiation which are known as local treatments, chemotherapy is almost always used as a systemic treatment, although it can also be used as local treatment (American Cancer Society, 2010c). This concept can be traced back to in the 1940s when the results of the first clinical trial involving nitrogen mustard treatment in patients with malignant lymphomas was first reported (Gilman and Philips, 1946).

Chemotherapy works by halting or slowing the growth of cancer cells which are known to grow and divide faster than normal cells. However, chemotherapy can cause side effects as it can also damage the normal cells since it is unable to differentiate between cancer cells and normal, healthy cells. Depending on the cancer type and stage, chemotherapy is able to cure cancer, control cancer or ease cancer symptoms (National Cancer Institute, 2010c).

Although chemotherapy is sometimes used as the sole treatment in cancers, it can also be used together with other cancer treatments such as surgery or radiation. Neo-adjuvant chemotherapy refers to the chemotherapy used before surgery or radiation to reduce the size of tumors while adjuvant chemotherapy is used to destroy the remaining cancer cells after surgery or radiation. Besides that, chemotherapy is also used in recurrent cancers and metastatic cancers (National Cancer Institute, 2010c).

2.5.2 Drug resistance

Although chemotherapy has lead to improvement in the survival rates and quality of life in cancer patients, drug resistance remains a major obstacle to improving the overall response and survival of cancer patients. Even though some tumors are intrinsically resistant towards chemotherapeutic drugs such as melanoma (Schadendorf *et al*., 1994), the development of resistance towards chemotherapeutic drugs (also known as acquired resistance) in cancer cells is a major cause of failure in chemotherapy (Selby, 1984). This is because, more often than not, tumor cells consist of a heterogeneous population of cells where some cells are drug-sensitive while others are drug-resistant. Thus, chemotherapy would sometimes kill only the drug-sensitive cells, leaving behind a proportion of drug-resistant cells. These cells would then proliferate and form a tumor, leading to cancer remission. Chemotherapy may not be as effective now as these remaining tumor cells are now mostly drug-resistant cells. Resistance to chemotherapy in cancer cells can occur at various levels (depicted in Figure 2.6), such as increased drug efflux and decreased drug influx, drug inactivation, alterations in drug target, processing of drug-induced damage and apoptosis evasion (Longley and Johnston, 2005).

This phenomenon is often observed in mono-targeted therapies as it allows the tumor cells to adapt to the particular drug treatment and changes its route of tumorigenesis. When this occurs, oncologists are forced to increase the dosage of chemotherapeutic drugs and in doing so, increase the risk of adverse side-effects of the drugs or switch to an alternative chemotherapy regimen. Therefore, the current treatments in cancers are now moving away from mono-targeted therapies and going into combination therapies involving the use of chemosensitizers or drugs with multiple modalities (Aggarwal *et al*., 2006; Abbruzzese and Lippman, 2004).

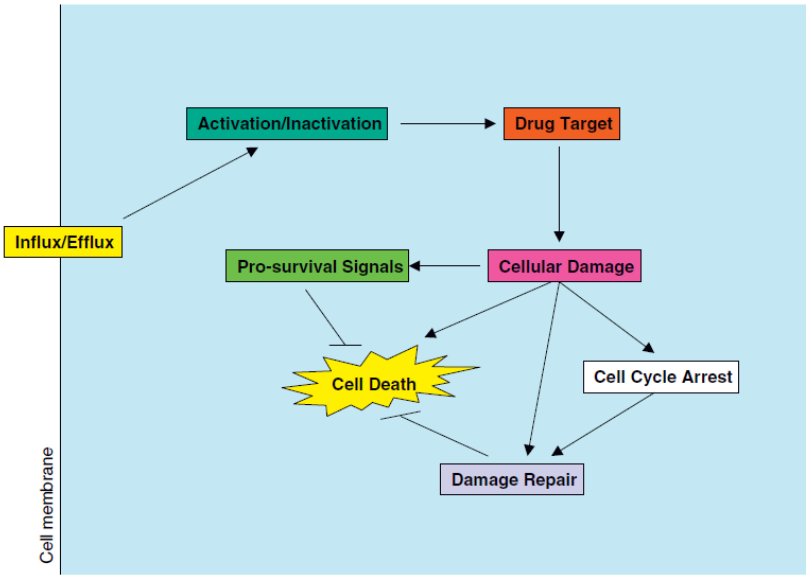

Figure 2.6: Mechanisms of drug resistance in cancer cells (figure adapted from Longley and Johnston, 2005).

2.5.3 Combination therapy

Combination therapies with multiple drugs or with multiple modalities have been introduced over the years in the treatment of cancers to improve the therapeutic efficacy without using an excessive quantity of either agent through a synergistic drug interaction. The use of combination therapies achieved better clinical results compared to mono-targeted therapies as it induces maximum cell kill and covers a broader spectrum of cells resistant to a specific drug present in a heterogeneous tumor cell population. Furthermore, this multi-targeted approach can also decelerate the development of drug resistant sub-clones of cells (Zoli *et al*., 2001).

The improvements in therapeutic efficacy using combination therapy on various cell lines have been reported in findings such as combinations using nedaplatin and irinotecan (Kanzawa *et al*., 2001); zoledronic acid and cisplatin (Ozturk *et al*., 2007); rapamycin and paclitaxel (Aissat *et al*., 2008) as well as genistein and cisplatin (Solomon *et al*., 2008). Furthermore, several drug combinations have also been

approved for use in the treatment of cancer by the U. S. Food and Drug Administration (FDA) such as topotecan hydrochloride in combination with cisplatin for treatment of Stage IVB recurrent or persistent cervical carcinoma (U.S. Food and Drug Administration, June 14, 2006); gemcitabine in combination with carboplatin for treatment of advanced ovarian cancer (U.S. Food and Drug Administration, July 14, 2006); as well as lapatinib in combination with letrozole for treatment of postmenopausal women with hormone receptor positive metastatic breast cancer that over-expresses HER2 receptor (U.S. Food and Drug Administration, January 29, 2010).

2.5.4 Combination analysis

Combination analysis is used to determine the effectiveness of two or more compounds when they are used together. This is done by determining whether the effects are synergistic (observed effects greater than expected effects), additive (not much difference between observed effects and expected effects) or antagonistic (observed effects lesser than expected effects). A synergistic effect is the desired interaction as it requires lesser dosage of anti-cancer drugs to achieve the same effect while antagonistic interaction should be avoided as it requires higher dosage of the anti-cancer drugs to achieve the same effect. Although there are many types of methods available to analyze the interactions between compounds when used in combination, isobologram analysis and combination index (CI) are among the more popular choices (Zhao *et al*., 2004).

In isobologram analysis, the concentrations of drugs A and B required to produce a defined single-agent effect (for example, the IC_{50}) when used as a standalone agent were first obtained. These values will then be placed on the x and y axes in a two-coordinate plot, corresponding to (C_A, 0) and (0, C_B), respectively. A line is then drawn

to connect these two points, known as the line of additivity. Following that, the concentrations of the drugs A and B when used in combination to produce the same effect are placed within the same plot, denoted as (C_A, C_B). The interaction between these two drugs are then determined. The interaction is synergistic, additive or antagonistic if the (C_A, C_B) is below, close to or above the line of additivity, respectively (Steel and Peckham, 1979).

As with the isobologram analysis, the CI analysis provides qualitative information on the nature of the drug interaction. The CI is calculated based on the formula below which provides a numerical value, thus providing a quantitative measurement to the extent of the drug interaction.

$$CI = \frac{C_{A,X}}{IC_{X,A}} + \frac{C_{B,X}}{IC_{X,B}}$$

The $C_{A,X}$ and $C_{B,X}$ are the concentrations of drugs A and B required to achieve x% effects when used in combination while $IC_{X,A}$ and $IC_{X,B}$ are the concentrations required by the drugs A and B to achieve the same effects when used as a standalone agent. The interaction is synergistic, additive or antagonistic if the CI is less than, equal to or more than 1, respectively (Zhao *et al.*, 2004).

2.5.5 Cisplatin

Cisplatin, also known as cis-dichlorodiammineplatinum [II] (CDDP), is an inorganic, square-planar coordination complex that is widely-used in treatment of various cancers such as ovarian, testicular, lung, cervical as well as head and neck carcinomas (Giaccone, 2000). The chemical structure of CDDP is illustrated in Figure 2.7.

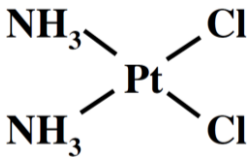

Figure 2.7: Chemical structure of cisplatin (CDDP) (figure adapted from Siddik, 2003).

This platinum-based anti-cancer drug is an alkylating-like agent, whereby the central platinum atom interacts covalently with DNA to form DNA-DNA interstrand and intrastrand crosslinks (Eastman, 1987). The ApG and GpG (where "p" is the phosphate linking the two bases) intrastrand crosslinks appears to be the major cytotoxic lesions formed, accounting for 85 to 90% of total DNA lesions (Kelland, 1993). These cytotoxic lesions are then detected by the damage recognition proteins, activating critical genes involved in signal transduction pathways which results in activation of apoptosis. Among the side-effects associated with cisplatin are nephrotoxicity, neurotoxicity, ototoxicity, electrolyte disturbance, nausea and vomiting (Page and Takimoto, 2004).

Just like many other anti-cancer agents, resistance towards cisplatin has been reported where cells failed to undergo apoptosis at clinically relevant doses or at achievable plasma drug concentrations. More often than not, the resistance mechanisms within a tumor is multifaceted (Richon *et al*., 1987) although the existence of a single

mechanism of resistance within a tumor is possible, but rare (Kelland *et al*., 1992). Studies have also shown that different resistance mechanisms exist between different cell lines (Kelland, 1993; Teicher *et al*., 1990). Among the mechanisms which have been found to contribute to cisplatin resistance are reduced drug uptake, enhanced drug efflux, increased inactivation by thiol-containing molecules, enhanced DNA damage repair, overexpression of HER-2/neu and PI3K/AKT as well as Ras/MAPK pathway, loss of p53 tumor suppressor function and inhibition of apoptosis (Siddik, 2003).

2.6 Natural compounds as anti-cancer agents

2.6.1 Overview

Natural compounds have been extensively used in the treatment of cancer and other diseases for many years. The importance of natural compounds in cancer treatment was reflected in a report by Newman *et al*., (2003), where it was found that 74% of FDA approved anti-cancer drugs from 1981 to 2002 were based on or mimics of natural compounds. A survey conducted by the National Cancer Institute (NCI) in USA found that more than two thirds of the anti-cancer drugs available are natural products, derivatives of natural products or mimic bioactive principles of natural products (Cragg *et al*., 2009).

Surprisingly, although most of the anti-cancer drugs are based on natural compounds, it is estimated that only 5% to 15% species of higher plants have been investigated for the presence of bioactive compounds (Balandrin *et al*., 1993), not including other natural sources such as animals, marine organisms and microorganisms. Thus, these remaining unexploited natural resources could potentially provide bioactive compounds which may be used alone or as adjuvant in combination chemotherapy to improve therapeutic efficacy by reducing drug-induced toxicities and/or overcoming drug resistance (Mahendale *et al*., 2005; Wang *et al*., 2005).

2.6.2 Plant-derived anti-cancer agents

Over the years, many plant-derived compounds have been successfully employed in the treatment of cancer. Among the most noteworthy examples is the vinca alkaloids vincristine isolated from the periwinkle *Catharanthus roseus*, which is endemic in the Madagascar rain forests (Noble, 1990). The cure rates for Hodgkin's disease and some forms of leukemia increased following the introduction of vincristine

(DeVita, 1970). Vinca alkaloids bind to tubulin and depolymerize the microtubules (Okouneva *et al*., 2003), leading to cell arrest in mitosis (Gidding *et al*., 1999). Besides the interaction with tubulins, its efficacy toward cancer cells is also due to other mechanisms (membrane-bound drug efflux transporters, signal transduction pathways and programmed cell death).

2.6.3 1'S-1'-Acetoxychavicol acetate

The 1'S-1'-acetoxychavicol acetate (ACA) used in this study is a natural compound isolated from *Alpinia conchigera* Griff. (Khalijah *et al*., 2010), also known in Malaysia as *lengkuas ranting*, *lengkuas kecil*, *lengkuas padang*, *lengkuas genting* or *chengkenam*. The *Alpinia* genus is the most widespread and taxonomically complex genus in Zingiberaceae family with 230 species found in tropical and sub-tropical Asia (Kress *et al*., 2005). The chemical structure of ACA is illustrated in Figure 2.8.

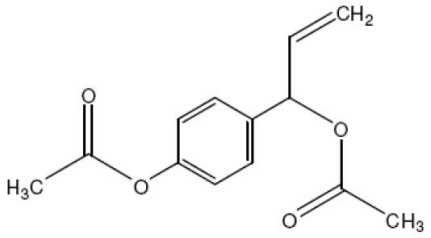

Figure 2.8: Chemical structure of 1'S-1'-acetoxychavicol acetate (ACA) (figure adapted from Khalijah *et al*., 2011)

The *Alpinia conchigera* is a herbaceous perennial, 2-5 feet tall plant found to be endemic in eastern Bengal and southwards toward Peninsular Malaysia and Sumatera (Burkhill, 1966). In the northern Peninsular Malaysia, the rhizomes from this plant are used in food flavoring while it is used as traditional medicine in the east coast. Its rhizomes are also used in Thai traditional medicine for relieving gastro-intestinal

disorders and in food preparation where they are used as condiments (Matsuda *et al*., 2005).

ACA has been shown to exhibit various biological activities in previous studies, such as anti-tumor (Itokawa *et al*., 1987), anti-inflammatory (Nakamura *et al*., 1998), anti-fungal (Janssen and Scheffer, 1985), anti-ulcer (Mitsui *et al*., 1985), anti-allergic (Matsuda *et al*., 2003), anti-oxidative (Kubota *et al*., 2001) and xanthine oxidase inhibitory activity (Noro *et al*., 1988). *In vivo* studies have also shown that ACA has potent chemopreventive effects on chemically induced tumor formation in mouse skin (Murakami *et al*., 1996), rat oral (Ohnishi *et al*., 1996), rat colon (Tanaka *et al*., 1997), rat esophagus (Kawabata *et al*., 2000), and Syrian hamster pancreas (Miyauchi *et al*., 2000).

Besides these *in vivo* observations, ACA was also found to be able to inhibit tumor promoter-induced Epstein-Barr virus activation (Kondo *et al*., 1993) and induce apoptosis in Ehrlich ascites tumor cells through modulation of polyamine metabolism and caspase-3 activation (Moffatt *et al*., 2000). Furthermore, ACA was also shown to inhibit the cellular growth of myeloid leukemic cells *in vitro* and *in vivo* through induction of apoptosis via mitochondrial- and Fas-mediated dual mechanism (Ito *et al*., 2004). More recently, it was also reported that ACA induced dose- and time-dependent cytotoxicity on various tumor cell lines without any adverse effects on normal cells (Khalijah *et al*., 2010).

2.7 MicroRNAs (miRNAs)

2.7.1 Overview

MicroRNAs (miRNAs) are small (~22 nucleotides long) non-coding RNA molecules that regulate genes post-transcriptionally (Lagos-Quitana *et al*., 2001). It is estimated that up to 1,000 unique miRNAs may be encoded in the vertebrate genome (Berezikov *et al*., 2005). The miRNAs are predicted to regulate the expression of around 60% of mammalian genes (Friedman *et al*., 2009) and are found in abundance in many human cell types (Lim *et al*., 2003), making them one of the largest classes of gene regulators.

Furthermore, studies have also shown that each miRNA is capable of regulating a large number of target mRNAs (Lim *et al*., 2005). It is postulated that an average miRNA regulates up to 100 different target mRNAs with more than 10,000 mRNAs directly regulated by miRNAs (Brennecke *et al*., 2005). It was also reported that miRNAs can reduce the protein levels without affecting the corresponding mRNA levels (Olsen, 1999), thus partially explained why some gene expression profiles based on mRNA do not always correlate with protein expression profiles (Kern, 2003).

Studies have also found miRNAs to be well conserved in eukaryotic organisms and are therefore thought to be a vital and evolutionarily ancient component of gene regulation (Grosshans and Slack, 2002; Tanzer and Stadler, 2004; Lee *et al*., 2007). Various studies conducted found that miRNAs have critical roles in cell proliferation and metabolism (Brennecke *et al*., 2003), developmental timing (Ambros, 2003; Reinhart *et al*., 2000), cell death (Baehrecke, 2003), hematopoiesis (Chen *et al*., 2004) and human tumorigenesis (Michael *et al*., 2003)

2.7.2 Naming convention for miRNAs

The convention for naming miRNAs followed certain criteria which have been described by Ambros *et al*., in 2003. An example of a miRNA name is hsa-miR-21. The first three letters in the miRNA name signify the organism. For example, hsa-miR-21 and mmu-miR-21 is used for miR-21 found in humans and mouse, respectively. On the other hand, the numbering of miRNAs is simply sequential based on their time of discovery, whereby miRNAs which are closely-numbered may not be related at all. Mature miRNA is designated as miR-21 in databases and literatures, while *mir-21* refers to the miRNA gene or the predicted stem-loop of the primary transcript. MiRNAs with identical mature sequences but expressed from distinct precursor sequences and genomic loci are designated as hsa-miR-21-1 and hsa-miR-21-2, while miRNAs with closely-related mature sequences are designated as hsa-miR-21a and hsa-miR-21b, indicating that they are expressed from precursors hsa-miR-21a and hsa-miR-21b, respectively.

Although one of the strands from miRNA duplex is usually degraded, studies sometimes identify two sequences of miRNAs which originated from the same precursor. When the relative abundances clearly indicated the predominantly expressed miRNA, the mature miRNA is designated as hsa-miR-21 (predominant product) or hsa-miR-21* (less dominant product from the opposite arm of the precursor). However, when data are not available to sufficiently distinguish the predominant miRNAs, names such as hsa-miR-21-5p (from the 5' arm) or hsa-miR-21-3p (from 3' arm) are used.

Even though most miRNAs followed this naming convention and several miRNAs which do not conform to this convention have since been renamed, miRNAs found in different organisms may have slightly different naming conventions, such as

plants and viruses. Besides these, miRNAs such as let-7 and lin-4 are also obvious exceptions to these naming conventions and their names have been retained for historical reasons. In addition to names, each miRNA has a unique accession number, the only stably identifier as miRNA names may be changed from time to time, depending on the circumstances. Hence, these accession numbers should be included as well, although they provide little biological meaning.

2.7.3 Biogenesis of miRNAs

The miRNAs are first transcribed from the miRNA genes by RNA polymerase II as long primary miRNA molecules (pri-miRNAs) (Lee *et al*., 2004) containing a 7-methyl guanosine cap at the 5' end and a poly(A) tail at the 3' end in the nucleus (Cai *et al*., 2004). The pri-miRNA is then processed into short hairpin RNAs of ~70 nucleotides long (known as pre-miRNA) by an RNase III enzyme, Drosha, and an essential cofactor DGCR8/Pasha (protein containing two double-stranded RNA binding domains) (Denli *et al*., 2004). They are subsequently processed into a 60-70 nucleotides pre-miRNA with 5' phosphate and 2 nucleotides overhangs at 3' before being transported into the cytoplasm by Exportin-5, in a RanGTP-dependent manner (Bohnsack *et al*., 2004).

In the cytoplasm, the pre-miRNA is cleaved by another RNase III enzyme, Dicer, together with the double-stranded RNA-binding protein TRBP and releases a ~22 nucleotides long double-stranded miRNA (Grishok *et al*., 2001; Winter *et al*., 2009). One of the strands from the miRNA duplex will be incorporated into RNA-induced silencing complex (RISC), while the complementary miRNA strand is usually rapidly degraded. The incorporated miRNA strand then binds to their target sequences which are generally found in the 3' UTR of target mRNA by the "seed" sequence of 2 to 7 nucleotides that is located near the 5' region of the miRNA, resulting in negative

regulation of gene expression (Lewis *et al*., 2005). This results in mRNA degradation if the miRNA binds to their target mRNA in perfect (or nearly perfect) complementarity or mRNA translational repression if the miRNA binds to their target mRNA in imperfect complementarity (Gregory *et al*., 2005). The biogenesis of miRNAs is illustrated in Figure 2.9.

However, recent evidences have suggested that miRNAs are also capable of binding to the 5' UTR of target mRNAs (Lytle *et al*., 2007) and can also up-regulate the translational of target mRNAs under specific conditions (Vasudevan *et al*., 2007). In addition, miRNAs can also bind to protein factors required for translation or alter the mRNA secondary structure, inhibiting protein translation (Ambros, 2001).

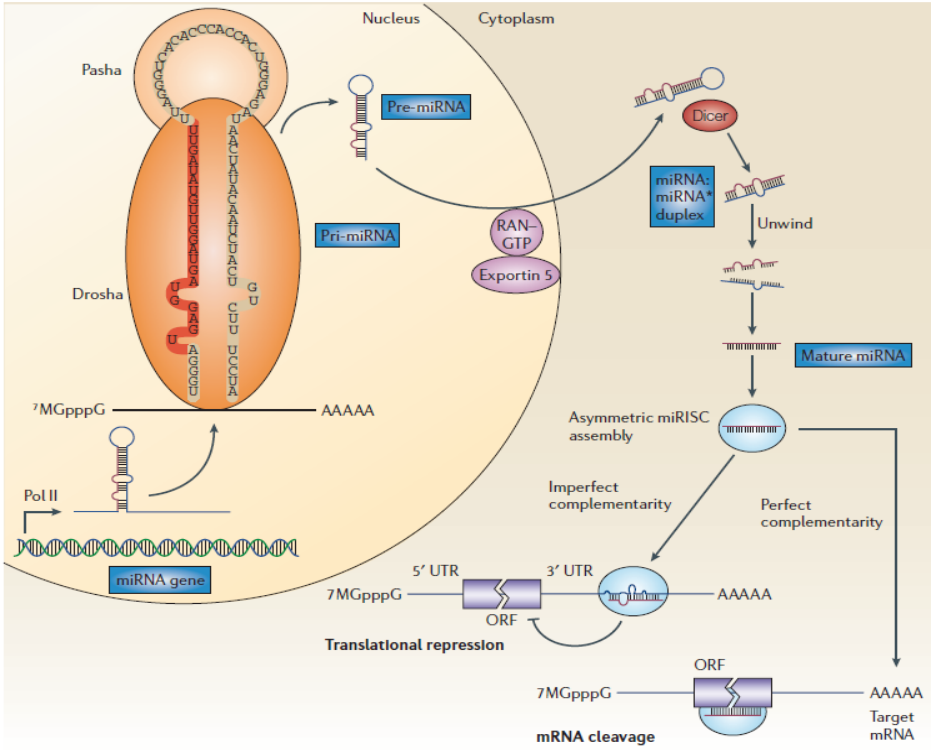

Figure 2.9: Biogenesis of microRNAs (figure adapted from Esquela-Kerscher and Slack, 2006)

2.7.4 MiRNAs and chemotherapy

With increasing evidences implicating miRNAs in malignancy and apoptosis in cancers, it is thought that miRNAs may also play a role in modulating sensitivity or resistance to cancer treatments such as chemotherapy. These possibilities have been investigated recently and several studies have demonstrated the potential roles played by miRNAs in modulating sensitivity or resistance to chemotherapy.

The correlations between miRNA expression patterns and potencies of various anti-cancer compounds have been demonstrated by Blower *et al*. (2007). In another study, the expressions of three miRNAs (let-7i, miR-16 and miR-21) were shown to significantly affect the potency of anti-cancer compounds with miR-21 having the most prominent effect on potency for the largest number of compounds. Besides that, *in silico* comparison of drug potencies with miRNA expression profiles across the NCI-60 cancer cell panel within the same study found that the expressions of 31 miRNAs have significant correlation with various anti-cancer drugs (Blower *et al*., 2008). Other than that, Meng *et al*. (2006) also demonstrated the role of two miRNAs (miR-21 and miR-200b) in modulating sensitivity or resistance to gemcitabine in cholagiocarcinoma. Additionally, two other miRNAs (miR-15b and miR-16) were also found to modulate sensitivity in five out of seven anti-cancer drugs tested in gastric cancer (Xia *et al*., 2008).

All together, these studies clearly suggest the potential roles of miRNAs in modulating sensitivity or resistance to chemotherapy. Thus, miRNAs could provide a new strategy to improve efficacy in cancer treatments, whereby miRNAs expression can be manipulated to increase sensitivity in cancer cells towards anti-cancer drug responses.

CHAPTER 3: MATERIALS AND METHODS

3.1 1'S-1'-acetoxychavicol acetate (ACA) and cisplatin (CDDP)

3.1.1 1'S-1'-acetoxychavicol acetate (ACA)

The ACA was provided by the Centre for Natural Product Research and Drug Discovery (CENAR), Department of Chemistry, University of Malaya. A stock solution of 1.0 M was made by dissolving the ACA in DMSO and kept at -20°C. The working solution was prepared by making aliquots of 0.01 M with DMSO as solvent and kept at -20°C until further use.

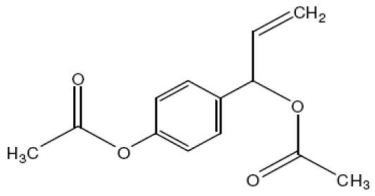

Figure 3.1: Chemical structure of 1'S-1'-acetoxychavicol acetate (ACA) (figure adapted from Khalijah *et al*., 2011)

3.1.2 Cisplatin (CDDP)

The working solution for cisplatin (CDDP) consisted of 5.0 mg of CDDP (Merck, Germany) in 1.0 ml of DMSO. The solution was mixed well and then stored at -20°C in the dark until further use.

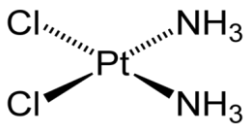

Figure 3.2: Chemical structure of cisplatin (CDDP) (figure adapted from Siddik, 2003).

3.2 Cell cultures

3.2.1 Cell lines and culture conditions

The human cervical carcinoma cells Ca Ski were obtained from the Faculty of Medicine, University of Malaya and cultured in 25.0 cm^2 cell culture flask (Nunc, Denmark) containing 5.0 ml of DMEM cell culture medium supplemented with 10.0% (v/v) FBS. The NP69 immortalized nasopharyngeal epithelial cells (NP69), which were used as normal cells control, were obtained from Cancer Research Initiatives Foundation (CARIF, Malaysia) and cultured in 25.0 cm^2 cell culture flask (Nunc, Denmark) containing 5.0 ml of KSFM cell culture medium supplemented with 5.0% (v/v) FBS. All cells were maintained in a carbon dioxide (CO_2) incubator (Memmert, Germany) at 37°C with 5.0% CO_2 and 95.0% humidified atmosphere.

3.2.2 Subculturing monolayer cell lines

The cell culture medium in the 25.0 cm^2 cell culture flask (Nunc, Denmark) was removed and discarded using an aspirator. The cell monolayer was then washed with 3.0 ml of 1× PBS to remove any remaining traces of cell culture medium which can inhibit the activity of trypsin-EDTA due to the presence of FBS. The solution in the cell culture flask was removed and discarded using an aspirator. Following that, 2.0 ml of 0.25% (v/v) trypsin-EDTA was added into the cell culture flask. The cell culture flask was then incubated at 37°C to facilitate cells detachment. The progress in the cells detachment was checked every few minutes by observing under the microscope (Nikon, Japan). Upon successful cells detachment, 2.0 ml of cell culture medium containing FBS was added into the cell suspension to inactivate the activity of trypsin-EDTA and any remaining cells were washed from the bottom of the cell culture flask. The cell suspension was then transferred into a labeled 15.0 ml centrifuge tube and centrifuged at 1,400 rpm for 6 min using Centrifuge 5702 (Eppendorf, Germany). The supernatant was

then discarded and the pellet was re-suspended in 6.0 ml of cell culture medium. Approximately 1.0 ml of the cell suspension was then added into 25.0 cm^2 cell culture flask (Nunc, Denmark) containing 4.0 ml of DMEM cell culture media supplemented with 10.0% (v/v) FBS. The cells were then maintained in a CO_2 incubator (Memmert, Germany) at 37°C with 5.0% CO_2 and 95.0% humidified atmosphere.

3.2.3 Cryopreservation of cell lines

Cells with 70-80% confluency were used in preparation for cryopreservation of cell lines. The cell culture medium was removed and discarded using an aspirator. The cell monolayer was then washed with 3.0 ml of 1× PBS to remove any remaining traces of cell culture medium. The solution in the cell culture flask was removed and discarded using an aspirator. Following that, 2.0 ml of 0.25% (v/v) trypsin-EDTA was added into the cell culture flask. The cell culture flask was then incubated at 37°C to facilitate cells detachment. The progress in the cells detachment was checked every few minutes by observing under the microscope (Nikon, Japan). Upon successful cells detachment, 2.0 ml of cell culture medium containing FBS was added into the cell suspension and any remaining cells were washed from the bottom of the cell culture flask. The cell suspension was then transferred into a labeled 15.0 ml centrifuge tube and centrifuged at 1,400 rpm for 6 min using Centrifuge 5702 (Eppendorf, Germany). The supernatant was then discarded and the pellet was re-suspended in 4.0 ml of cell freezing medium containing cell culture medium supplemented with 20.0% (v/v) FBS and 5.0% (v/v) DMSO as cryoprotectant agent. Aliquots of 1.5 ml of cell suspension in 2.0 ml cryovials were made and frozen gradually (4°C for 3 h followed by -20°C for 3 h) before finally being stored in liquid nitrogen at -196°C for long term storage.

3.2.4 Thawing of cryopreserved cell lines

Cryopreseved cells were removed from liquid nitrogen and thawed at 37°C for 5 min (or until only a small piece of ice was left). The cell suspension was then added into two 25.0 cm^2 cell culture flasks (Nunc, Denmark) containing 4.0 ml of cell culture media supplemented with 20.0% (v/v) FBS. The cells were then maintained in a CO_2 incubator (Memmert, Germany) at 37°C with 5.0% CO_2 and 95.0% humidified atmosphere. Upon successful cells attachment, the old cell culture medium was then replaced with fresh cell culture medium.

3.2.5 Cell count

The cell suspension (as described in Section 3.2.1.2) was gently mixed and 20.0 µl of the cell suspension was aliquoted into a 1.5 ml microcentrifuge tube containing 20.0 µl of trypan blue solution. The solution was mixed well and allowed to stand for 3 min. After that, 10.0 µl of the mixture was removed and load onto a clean hemacytometer for cell counting under the microscope (Nikon, Japan) where dead cells stained blue while viable cells appeared as bright spheres. After cell counting, the actual concentration of the cell suspension (number of viable cells/ml) was determined using the following equation:

$$\frac{\text{(Total number of viable cells) (Dilution factor)}}{\text{(Proportion of chamber counted) (Volume of chamber)}} \times 1{,}000$$

From the actual concentration calculated, the cells were then diluted with cell culture medium to obtain the desired concentration.

3.3 MTT cell viability assays

First, the number of cells in the cell suspension was counted (described in Section 2.2.3) and plated at 1.0×10^4 cells/well in a 96-wells plate (Nunc, Denmark). The cells were then incubated in a CO_2 incubator (Memmert, Germany) at 37°C with 5% CO_2 and 95% humidified atmosphere overnight for cells re-attachment. Controls included in each plate were wells containing cells in gradient concentration for standard control, wells containing cells for solvent control and wells with cell culture medium alone to provide blank for absorbance readings. Once the cells have re-attached to the surface, cells were treated with standalone ACA, standalone CDDP or ACA in combination with CDDP at various concentrations and incubation hours. At the end of each incubation period, 20.0 µl of MTT solution was added to each well. The plate was then incubated at 37°C for 2 h and viewed periodically under the microscope (Nikon, Japan) for the presence of purple precipitate. After that, media containing the excess MTT solution was removed and 200.0 µl of DMSO was added to each well. The plate was then left in the dark at room temperature to allow the formazan crystals to dissolve. Once the formazan crystals were dissolved, results were obtained using microtiter plate reader (Tecan Sunrise®, Switzerland) which detects absorbance wavelength at 570 nm with reference wavelength at 650 nm. The combined effects of ACA and CDDP were evaluated using isobologram and combination index (CI) values to determine the interactions between ACA and CDDP. CI > 1.0 indicates an antagonistic interaction, CI = 1.0 indicates an additive interaction and CI < 1.0 indicates a synergistic interaction between two drugs (adapted from Zhao *et al*., 2004).

3.4 Total RNA extraction and quality control

3.4.1 Total RNA extraction

Cells were first plated in 75.0 cm^2 cell culture flask (Corning, USA) containing 15.0 ml of DMEM cell culture medium and incubated in a CO_2 incubator (Memmert, Germany) at 37°C with 5% CO_2 and 95% humidified atmosphere overnight. The cell culture medium was removed and discarded using an aspirator. Next, 15.0 ml of DMEM cell culture medium without the addition of FBS was then added into the cell culture flasks and the cells were treated with various concentrations of the drug (as summarized in Table 3.1) for 2 h. After 2 h, the total RNA from each flask was extracted using TRIZOL® Reagent (Invitrogen, USA) according to the manufacturer's protocol. The cells were first trypsinized and pelleted (as described in Section 3.2.1.2). Supernatant was then discarded and 1.0 ml of TRIZOL® Reagent (Invitrogen, USA) was added to the pellet whereby the cells were lyzed in TRIZOL® Reagent (Invitrogen, USA) through repetitive pipetting. The homogenized samples were then incubated at room temperature for 5 min to allow for complete dissociation of nucleoprotein complexes. Next, 200.0 µl of chloroform was added and the tubes were shaken by hand vigorously for 15 s and incubated at room temperature for 2 min. This was followed by centrifugation at 12,000 × *g* for 15 min at 4°C. After that, the colorless upper aqueous phase was transferred into a new 1.5 ml microcentrifuge tube and 500.0 µl of isopropanol was added. The samples were then incubated at room temperature for 10 min and centrifuged at 12,000 × *g* for 10 min at 4°C. After centrifugation, the RNA precipitate formed a gel-like pellet on the bottom side of the tubes. The supernatant was discarded and the RNA pellet was washed with 1.0 ml of 75% ethanol. The samples were then mixed by vortexing followed by centrifugation at 7,500 × *g* for 5 min at 4°C. The supernatant was discarded and the RNA pellet was air-dried. The RNA pellet was then dissolved in RNAse-free

water by passing the solution through a pipette tip several times and incubated for 10 min at 58°C. All RNA samples were stored at -30°C until further use.

Table 3.1: Summary of experimental setup used in this study indicating treatment groups with biological replicates.

Sample type	ACA concentration (µM)	CDDP concentration (µM)	Number of Biological replicates
Untreated	0	0	3
Standalone ACA	6.0	0	3
Standalone CDDP	0	53.3	3
ACA in combination with CDDP	3.0	13.0	3

3.4.2 RNA quality control

The concentration, integrity and purity of the RNA extracted were checked using UV spectrophotometry and Agilent RNA 6000 Nano Kit (Agilent Technologies, USA).

3.4.2.1 RNA analysis using UV spectrophotometry

The purity of the extracted RNA was checked using UV spectrophotometer. The 10 mM Tris-Cl, pH 7.5, was used as a blank before the absorbance readings were taken using Eppendorf Biophotometer (Eppendorf, Germany). The extracted RNA samples from Section 3.2.3.1 was diluted at ratio of 1/50 in 10 mM Tris-Cl, pH 7.5, before the absorbance readings were obtained. The purity of the extracted RNA was determined using the ratio of A_{260nm}/A_{280nm}, A_{260nm}/A_{230nm} and A_{320nm}. A ratio of 1.8 – 2.0 for A_{260nm}/A_{280nm} and A_{260nm}/A_{230nm} as well as A_{320nm} value of 0 indicates absence of contaminants which could possibly interfere and/or inhibit with the downstream experiments.

3.4.2.2 RNA analysis using Agilent RNA 6000 Nano Kit

The concentration and integrity of the extracted RNA was checked using Agilent RNA 6000 Nano Kit and analyzed with Agilent 2100 Bioanalyzer according to the manufacturer's protocol (Agilent Technologies, USA). The Agilent RNA 6000 Nano gel matrix was prepared by adding 550.0 µl of gel matrix into the top receptacle of a spin column and centrifuged at 1,500 × *g* for 10 min. The mixture containing 1.0 µl of RNA 6000 Nano dye concentrate and 65.0 µl of aliquoted of filtered gel matrix was vortexed vigorously. This mixture was then centrifuged at 13,000 × *g* for 10 min and used within the same day. A total of 9.0 µl of the gel-dye mix was then added into the bottom of each well marked ladder on RNA 6000 Nano chips (Agilent Technologies, USA). After that, 5.0 µl of the RNA 6000 Nano marker was added into each well marked ladder and sample, and an additional 1.0 µl of RNA ladder was added into well marked ladder. A total of 1.0 µl of extracted RNA samples from Section 3.2.3.1 was heat denatured at 70°C for 2 min before adding each sample well. The RNA 6000 Nano chips (Agilent Technologies, USA) was then vortexed on IKA vortexer (Agilent Technologies, USA) at 2,400 rpm for 1 min before being analyzed on Agilent 2100 Bioanalyzer (Agilent Technologies, USA). The quality of RNA samples were then assessed based on 28S/18S rRNA ratios, whereby a ratio of 2.0 indicates relatively intact RNA, as well as by RNA integrity number (RIN) value, whereby RIN value of 0 indicates highly degraded RNA sample while RIN value of 10 indicates highly intact RNA sample.

3.5 MiRNA microarray

3.5.1 FlashTag™ RNA labeling

The labeling of extracted RNA samples from Section 3.2.3.1 was performed using FlashTag™ Biotin RNA Labelling Kit for Affymetrix® GeneChip® miRNA Arrays (Genisphere, USA) according to the manufacturer's protocol. A total of 1.0 µg of total RNA was used for a brief tailing reaction followed by ligation of the biotinylated signal molecule to the target RNA sample. The volume of RNA was adjusted to 8.0 µl with nuclease-free water before adding 2.0 µl of RNA Spike Control Oligos and put on ice. The following components listed in Table 3.2 were then mixed gently with the 10.0 µl RNA/Spike Control Oligos, for a total volume of 15.0 µl. The mixture was centrifuged briefly and then incubated at 37°C for 15 min for poly (A) tailing. After 15 min, the 15.0 µl of tailed RNA was centrifuged briefly and placed on ice. A total of 4.0 µl of 5× FlashTag Ligation Mix Biotin and 2.0 µl of T4 DNA ligase was added to the tailed RNA and incubated at 25°C for 30 min. The reaction was then stopped by adding 2.5 µl Stop Solution. A total of 2.0 µl of the biotin-labeled sample was removed for ELOSA QC Assay while the remaining 21.5 µl sample was stored at -20°C, prior to hybridization on GeneChip® miRNA Array (Affymetrix, USA).

Table 3.2: Setup for FlashTag™ RNA labeling

Component	Volume per sample (µl)
10× Reaction Buffer	1.5
$MnCl_2$ (25 mM)	1.5
Diluted ATP Mix (1:500)	1.0
PAP Enzyme	1.0
Total volume	5.0

3.5.2 ELOSA quality control assays

The Enzyme Linked Oligosorbent Assay (ELOSA) is performed to confirm the successful labeling of the RNA samples by the FlashTag™ Biotin RNA Labelling Kit for Affymetrix® GeneChip® miRNA Arrays (Genisphere, USA) and was carried out according to the manufacturer's protocol. The ELOSA Spotting Oligos was first diluted with 1× PBS at ratio of 1:50 before 75.0 µl of the diluted ELOSA Spotting Oligos was added to each well of the Flat bottom Immobilizer™ Amino strip (Genisphere, USA). The strip was then sealed with adhesive plate sealer and incubated at 4°C overnight. Following overnight incubation, the ELOSA Spotting Oligos was removed and the wells were washed twice with 1× PBS, 0.02% Tween-20. The wells were then blot dried and 150.0 µl of 5% BSA in 1× PBS was added to each well. The wells was then covered and incubated for 1 h at room temperature. After that, the BSA blocking solution was removed and 52.5 µl of hybridization solution (as listed in Table 3.3) was added into designated well. The wells were then covered and incubated for 1 h at room temperature. The hybridization solution was then removed and wells were washed vigorously for 3 times with 1× PBS, 0.02% Tween-20 and blot dried. A total of 75.0 µl of diluted SA-HRP in 5% BSA in 1× PBS (1:6,000) was added into each well. The wells were then covered and incubated for 30 min at room temperature. The SA-HRP was then removed and wells were washed vigorously for 3 times with 1× PBS, 0.02% Tween-20 and blot dried before 100.0 µl of TMB Substrate was added into each well. The wells were then covered and incubated for 30 min at room temperature, in the dark. A successful ELOSA quality control assay was determined by the presence of blue substrate color, which indicates a positive result and may be used as a qualitative result.

Table 3.3: Setup for hybridization solution for ELOSA quality control assays

Component	Volume per sample (µl)
FlashTag™ Biotin-labeled RNA sample or ELOSA Negative Control or ELOSA Positive Control	2.0
5× SSC, 0.05% SDS, 0.005% BSA	48.0
25% Dextran sulfate	2.5
Total volume	52.5

3.5.3 Hybridization of Affymetrix arrays

The 20× Eukaryotic Hybridization Controls was first completely thawed and heated up at 65°C for 5 min. The following components listed in Table 3.4 were then added to the 21.5 µl biotin-labeled sample, to prepare the array hybridization cocktail. The array hybridization cocktail was then incubated at 99°C for 5 min, followed by 45°C for 5 min. A total of 100.0 µl of the array hybridization cocktail was then aspirated and injected into the GeneChip® miRNA Array (Affymetrix, USA). Both septa on the arrays were covered with 1/2" Tough-Spots to minimize evaporation and/or prevent leaks before being incubated in the GeneChip® Hybridization Oven 640 (Affymetrix, USA) at 48°C and 60 rpm for 16 h.

Table 3.4: Setup for array hybridization cocktail

Component	Volume per sample (µl)
2× Hybridization Mix	50.0
Nuclease-free water	10.0
Deionized formamide	5.0
DMSO	10.0
20× Eukaryotic Hybridization Controls	5.0
Control Oligonucleotide B2 (3 nM)	1.7
Total volume	81.7

3.5.4 Washing and staining of Affymetrix arrays

Following 16 h of hybridization, the arrays were removed from the hybridization oven and the hybridization cocktail was replaced with 100.0 µl of Array Holding Buffer. The arrays were allowed to equilibrate to room temperature before being washed and stained by GeneChip® Fluidics Station 450 (Affymetrix, USA) according to the manufacturer's protocol, which is summarized in Table 3.5.

Table 3.5: Summary of washing and staining protocol for each array

Protocol	Description
Post Hyb Wash #1	10 cycles of 2 mixes/cycle with Wash Buffer A at 25°C
Post Hyb Wash #2	8 cycles of 15 mixes/cycle with Wash Buffer B at 50°C
1st Stain	Stain the probe array for 10 min with Stain Cocktail 1 at 25°C
Post Wash Stain	10 cycles of 4 mixes/cycle with Wash Buffer A at 30°C
2nd Stain	Stain the probe array for 10 min with Stain Cocktail 2 at 25°C
3rd Stain	Stain the probe array for 10 min with Stain Cocktail 1 at 25°C
Final Wash	15 cycles of 4 mixes/cycle with Wash Buffer A at 35°C
Array Holding Buffer	Fill the probe with Array Holding Buffer

3.5.5 Statistical and miRNA expression analysis

The data obtained from the miRNA microarray was first analyzed with miRNA QC Tool v1.0.33.0 (Affymetrix, USA) for data summarization, normalization and quality control. The five probe sets (spike in-control-2_st, spike in-control-23_st, spike in-control-29_st, spike in-control-31_st and spike in-control-36_st) were confirmed to have signal-background mean intensities of more than 1,000 units before the data was exported into Partek® Genomics Suite™ v6.5 (Partek Inc., USA) for further analysis. Data was first normalized using Robust Multichip Average (RMA) which consists of three steps: background adjustment, quantile normalization and summarization. Data obtained was then filtered using fold-change value of more than or equal to 1.5, and *p* value of less than or equal to 0.05 to generate a list of differentially expressed miRNAs as compared to untreated controls.

3.6 Validation of miRNA microarray data

3.6.1 Reverse transcription PCR

A total of 5.0 ng of extracted total RNA samples from Section 3.2.3.1 was used for reverse transcriptase reactions using TaqMan® MicroRNA Reverse Transcription Kit (Applied Biosystems, USA). The volumes for each PCR reaction were prepared according to Table 3.6 with the total volume of reaction mixture per tube being 10.0 µl. The 10.0 µL reactions were incubated for 16°C for 30 min, 42°C for 30 min, 85°C for 5 min, and then held at 4°C using C1000™ Thermal Cycler (Bio-Rad Laboratories, USA).

Table 3.6: PCR setup for reverse transcription PCR

Component	Volume per sample (µl)
Stem-loop RT primer	2.0
10× RT Buffer	1.0
dNTP (100 mM)	0.1
MultiScribe™ Reverse Transcriptase (50 U/µL)	0.67
RNase inhibitor (20 U/µL)	0.13
Total RNA template (0.5 ng/µL)	3.33
Nuclease-free water	2.77
Total volume	10

3.6.2 Real-time PCR amplification and quantitation

The cDNA obtained from reverse transcription PCR was subsequently used for target amplification using TaqMan® MicroRNA Assays (Applied Biosystems, USA). The volumes for each PCR reaction were prepared according to Table 3.7 with the total volume of reaction mixture per tube being 10.0 µl. Reactions were incubated at 50°C for 2 min and then 95°C for 20 s followed by 40 cycles at 95°C for 3 s and 60°C for 20 s. PCR reactions were run on a Bio-Rad CFX96™ Real-Time PCR Detection System (Bio-Rad Laboratories, USA) and analyzed using Bio-Rad CFX Manager v1.6 (Bio-Rad Laboratories, USA). The U6 small nuclear RNA was used as an internal control to normalize RNA input. The fold-change was calculated using the $2^{-\Delta\Delta Ct}$ method (as

described previously by Livak and Schmittgen, 2001) and presented as fold-expression changes relative to untreated controls after normalization to endogenous controls.

Table 3.7: PCR setup for real-time PCR amplification and quantitation

Component	Volume per sample (µl)
2× TaqMan® Fast Advanced Master Mix	5.0
TaqMan® 20× Primer Probe Assay	0.5
RT product	0.67
Nuclease-free water	3.83
Total volume	10

3.7 Bioinformatic analyses of miRNA gene targets

The putative gene targets of miRNAs were predicted using TargetScanHuman v5.2 at http://www.targetscan.org/vert_50/ (Lewis *et al*., 2005). Putative gene targets with total context scores less than or equal to 0 were subsequently selected for gene-annotation enrichment analysis and results obtained were then filtered for tumorigenesis and cancer-related pathways found in Kyoto Encyclopedia of Genes and Genomes (KEGG) pathway database using Database for Annotation, Visualization and Integrated Discovery (DAVID) v6.7 at http://david.abcc.ncifcrf.gov/ (Huang *et al*., 2009).

3.8 Statistical analysis

All experiments were carried out in triplicate and presented as mean values ± standard deviation. Student's *t*-test was used to determine the statistical significance of the results whereby a p value of less than or equal to 0.05 was considered significant. Pearson correlation coefficient was used to determine the association between miRNA microarray data and qRT-PCR.

CHAPTER 4: RESULTS

4.1 Cytotoxicity assay

4.1.1 Cytotoxic effects of ACA and CDDP on Ca Ski cells

The MTT cell viability assay which measures the mitochondrial dehydrogenases activity in viable cells was used to investigate the cytotoxic effects of ACA and/or CDDP on Ca Ski cells and also the mode of cytotoxicity, whether it is dose- or time-dependent. The data obtained from MTT assays was also used to determine the IC_{50} values, which are determined based on the concentration of ACA or CDDP required to kill 50% of the cell population, to be used for subsequent experiments.

The cytotoxic effects of standalone ACA and standalone CDDP on Ca Ski cells was first assessed with MTT cell viability assay. Cells were treated with concentrations of ACA ranging from 0 to 12.0 μM or CDDP ranging from 0 to 200.0 μM and with incubation hours ranging from 12 to 48 h. Results obtained for standalone ACA and standalone CDDP are shown in Figure 4.1 and Figure 4.2, respectively.

Based on both figures, it was observed that total viable cells declined consistently with increasing concentrations of ACA or CDDP at each incubation period. Furthermore, a decline of total viable cells was also observed with increasing incubation periods at constant ACA or CDDP concentrations.

Together, results showed that both ACA and CDDP induce dose- and time-dependent cytotoxicity in Ca Ski cells when used as standalone agents. The IC_{50} values of ACA and CDDP at 24 h are 6.0 ± 0.15 μM and 53.3 ± 0.64 μM, respectively and these values were used for subsequent experiments.

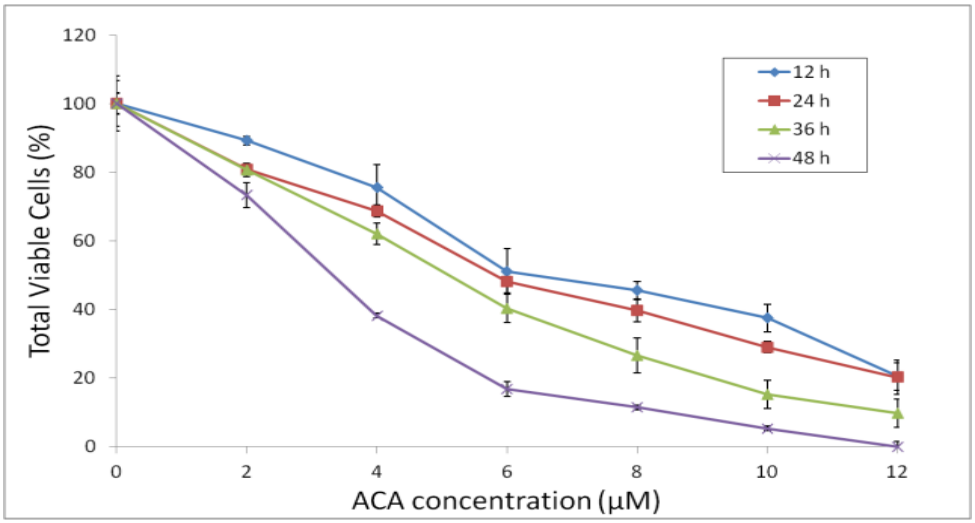

Figure 4.1: Comparative dose-response curve for standalone ACA on Ca Ski cells at various concentrations and incubation hours.

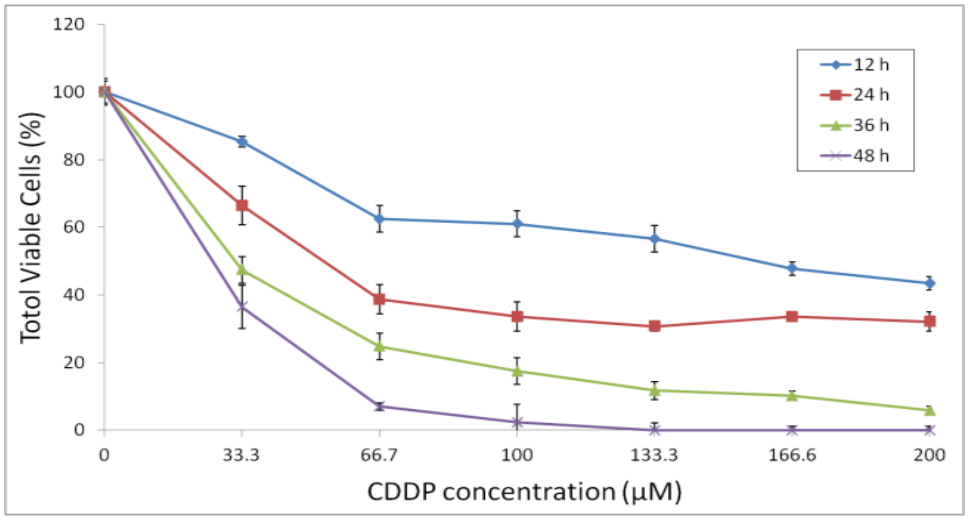

Figure 4.2: Comparative dose-response curve for standalone CDDP on Ca Ski cells at various concentrations and incubation hours.

4.1.2 Cytotoxic effects of ACA in combination with CDDP on Ca Ski cells

The combined effects of ACA and CDDP when used in combination on Ca Ski cells were next evaluated using MTT cell viability assay. A total of four different

combination regimens which employed various concentrations of ACA and CDDP were carried out (summarized in Table 4.1) and results are shown in Figure 4.3.

All four combination regimens resulted in decrease of total cell viability with increasing concentrations of ACA or CDDP, as shown in Figure 4.3. The IC_{50} values for each combination was calculated and compared to the IC_{50} values obtained earlier for ACA and CDDP when used as a standalone agent (summarized in Table 4.2).

The IC_{50} value for ACA was reduced from 6.0 μM when used as a standalone agent to 2.5 μM and 4.8 μM in simultaneous treatment with CDDP at constant concentration of 24.0 μM and ACA (0 - 12.0 μM) for 24 h and sequential pre-treatment with CDDP at 24.0 μM for 12 h followed by ACA (0 - 12.0 μM) for 24 h, respectively. Similarly, a reduction in the IC_{50} value of CDDP was also observed, whereby it was reduced from 53.3 μM when used as a standalone agent to 13.0 μM in simultaneous treatment with ACA at constant concentration of 3.0 μM and CDDP (0 - 100.0 μM) for 24 h and 13.3 μM in sequential pre-treatment with ACA at 3.0 μM for 12 h followed by CDDP (0 - 100.0 μM) for 24 h.

Overall, combinations which employed simultaneous treatment with ACA at constant concentration of 3.0 μM and CDDP (0 - 100.0 μM) for 24 h for 24 h and sequential pre-treatment with ACA at 3.0 μM for 12 h followed by CDDP (0 - 100.0 μM) for 24 h exhibited the highest percentage of reduction among the four combinations tested with a reduction of 75.6% and 75.0%, respectively. A reduction of 58.3% was seen in simultaneous treatment with CDDP at constant concentration of 24.0 μM and ACA (0 - 12.0 μM) for 24 h while only a 20.0% reduction was observed in

sequential pre-treatment with CDDP at 24.0 µM for 12 h followed by ACA and ACA (0 - 12.0 µM) for 24 h.

Table 4.1: Summary of combination regimens employed for MTT cell viability assay to evaluate the combined effects of ACA and CDDP on Ca Ski cells.

Combination	Treatment regimen
C1	Simultaneous treatment with ACA at constant concentration of 3.0 µM and CDDP (0 - 100.0 µM) for 24 h
C2	Simultaneous treatment with CDDP at constant concentration of 24.0 µM and ACA (0 - 12.0 µM) for 24 h
C3	Sequential pre-treatment with ACA at 3.0 µM for 12 h followed by CDDP (0 - 100.0 µM) for 24 h
C4	Sequential pre-treatment with CDDP at 24.0 µM for 12 h followed by ACA (0 - 12.0 µM) for 24 h

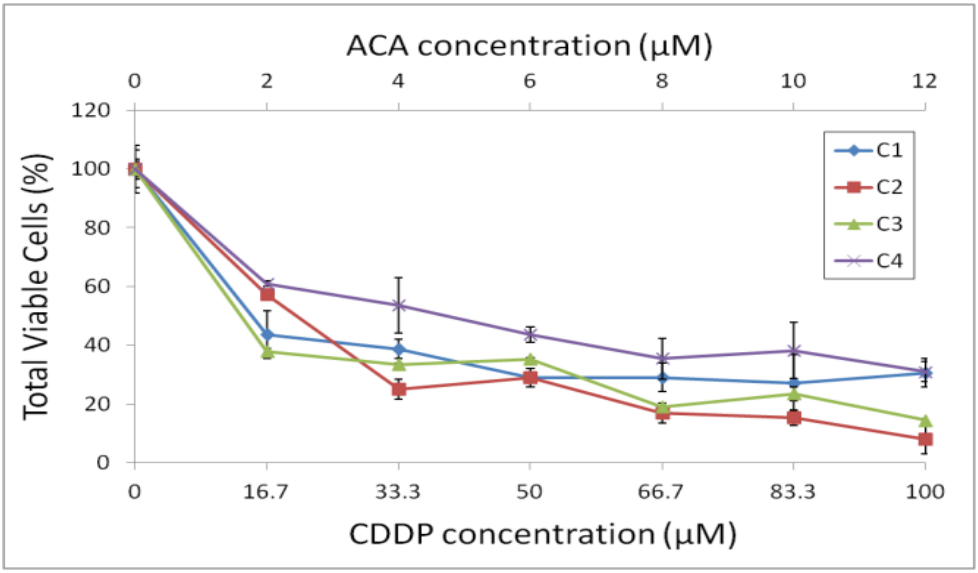

Figure 4.3: Comparative dose-response curve for ACA and CDDP on Ca Ski cells for different combinations following 24 h exposure.

† C1: Simultaneous treatment with ACA at constant concentration of 3.0 µM and CDDP (0 - 100.0 µM) for 24 h; C2: Simultaneous treatment with CDDP at constant concentration of 24.0 µM and ACA (0 - 12.0 µM) for 24 h; C3: Sequential pre-treatment with ACA at 3.0 µM for 12 h followed by CDDP (0 - 100.0 µM) for 24 h; C4: Sequential pre-treatment with CDDP at 24.0 µM for 12 h followed by ACA (0 - 12.0 µM) for 24 h.

Table 4.2: Summary of IC_{50} values for standalone ACA, standalone CDDP and ACA in combination with CDDP at various concentrations following 24 h exposure.

Combination	ACA (μM)	CDDP (μM)
Standalone ACA	6.0	-
Standalone CDDP	-	53.3
C1	3.0	13.0
C2	2.5	24.0
C3	3.0	13.3
C4	4.8	24.0

† C1: Simultaneous treatment with ACA at constant concentration of 3.0 μM and CDDP (0 - 100.0 μM) for 24 h; C2: Simultaneous treatment with CDDP at constant concentration of 24.0 μM and ACA (0 - 12.0 μM) for 24 h; C3: Sequential pre-treatment with ACA at 3.0 μM for 12 h followed by CDDP (0 - 100.0 μM) for 24 h; C4: Sequential pre-treatment with CDDP at 24.0 μM for 12 h followed by ACA (0 - 12.0 μM) for 24 h.

4.2 Combination analysis

Although the MTT cell viability assays clearly showed that ACA in combination with CDDP was able to reduce the percentage of total viable cells and IC_{50} values, it was still necessary to determine the interactions involved as drugs with overtly similar mechanisms might results in antagonistic effects. Hence, isobologram and combination index, the two most popular methods for evaluating drug interactions in combination chemotherapy were used in this study.

Both isobologram (Figure 4.4) and combination index (Table 4.3) showed that synergistic relationships were observed when cells were treated with ACA and CDDP simultaneously as well as sequentially over 24 h. However, a shift towards an antagonistic relationship was observed when a sequential 12 h pre-treatment with CDDP was followed by ACA for 24 h. Taken together, these results suggest that ACA

acts as a potential chemosensitizer which sensitizes Ca Ski cells through undetermined mechanisms prior to CDDP exposure, thereby potentiating the cytotoxic effects of CDDP.

Since C1 (simultaneous treatment with ACA at constant concentration of 3.0 μM and CDDP (0 -100.0 μM) for 24 h) exhibited the lowest CI value among those combinations tested, it was subsequently selected for downstream experiments in identifying miRNAs involved in modulating response towards ACA and/or CDDP.

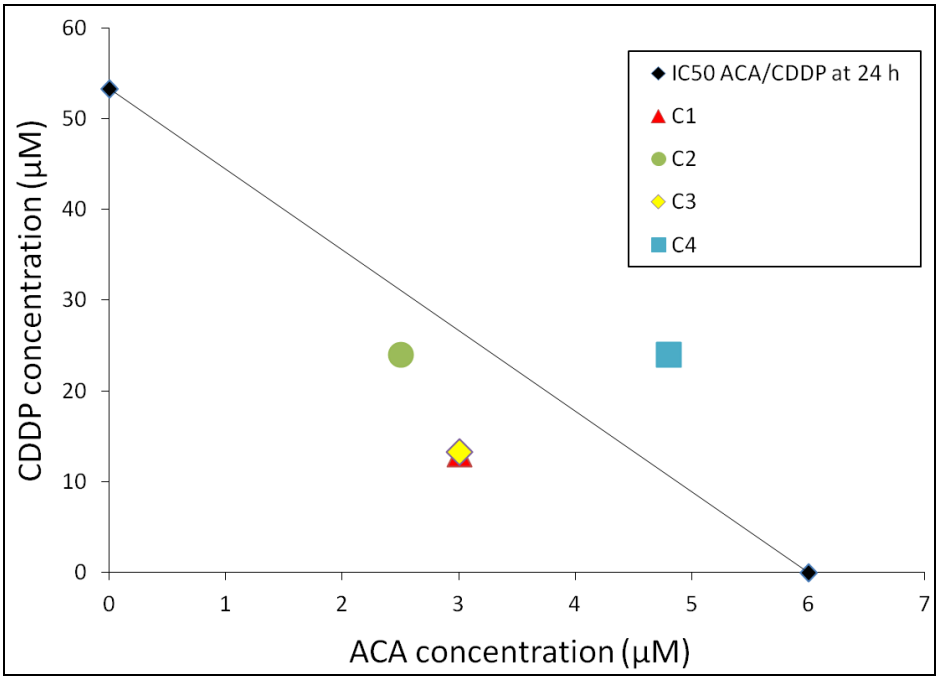

Figure 4.4: Isobologram analysis of ACA in combination with CDDP.

† C1: Simultaneous treatment with ACA at constant concentration of 3.0 μM and CDDP (0 - 100.0 μM) for 24 h; C2: Simultaneous treatment with CDDP at constant concentration of 24.0 μM and ACA (0 - 12.0 μM) for 24 h; C3: Sequential pre-treatment with ACA at 3.0 μM for 12 h followed by CDDP (0 - 100.0 μM) for 24 h; C4: Sequential pre-treatment with CDDP at 24.0 μM for 12 h followed by ACA (0 - 12.0 μM) for 24 h.

Table 4.3: Combination index analysis of ACA in combination with CDDP.

Combination	ACA (μM)	CDDP (μM)	CI value	Relationship
C1	3.0	13.0	0.74 ± 0.01	Synergistic
C2	2.5	24.0	0.87 ± 0.02	Synergistic
C3	3.0	13.3	0.75 ± 0.02	Synergistic
C4	4.8	24.0	1.25 ± 0.05	Antagonistic

† C1: Simultaneous treatment with ACA at constant concentration of 3.0 μM and CDDP (0 - 100.0 μM) for 24 h; C2: Simultaneous treatment with CDDP at constant concentration of 24.0 μM and ACA (0 - 12.0 μM) for 24 h; C3: Sequential pre-treatment with ACA at 3.0 μM for 12 h followed by CDDP (0 - 100.0 μM) for 24 h; C4: Sequential pre-treatment with CDDP at 24.0 μM for 12 h followed by ACA (0 - 12.0 μM) for 24 h.

4.3 Normal cells and solvent control

4.3.1 Cytotoxic effects of ACA and CDDP on normal cells

The cytotoxic effects of ACA and CDDP were next assessed on normal cells to ensure that ACA does not induce significant cytotoxicity in normal cells, a pre-requisite in studies involving natural compounds, while CDDP was included to obtain a comparison in the cytotoxicity levels between ACA and CDDP on the normal cells. In this study, the NP69 immortalized nasopharyngeal epithelial cells were used as normal cell control and cells were treated with concentrations of ACA ranging from 0 to 12.0 μM or CDDP ranging from 0 to 200.0 μM for 24 h. The cytotoxic effect of the combination which was to be used for subsequent downstream experiments was also tested on NP69 cells to ensure that it does not induce significant effects.

Figure 4.5 showed that while CDDP reduced the total viable cells to 45% at the highest concentration, the total viable cells following treatment with ACA was maintained at 75%. Besides that, Figure 4.6 showed that total viable cells remained at 80% following treatment using this combination.

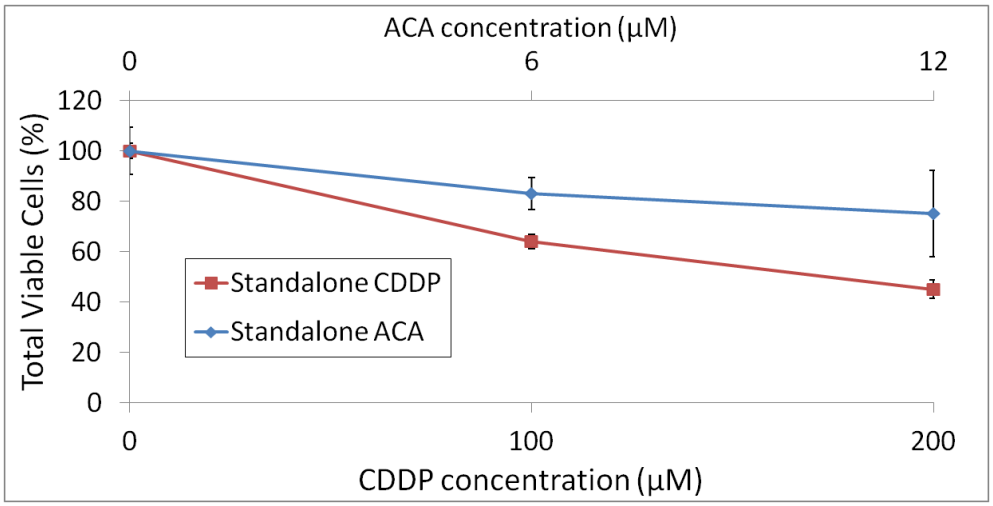

Figure 4.5: Comparative dose-response curve at various concentrations of standalone ACA (0 - 12.0 µM) and CDDP (0 - 200.0 µM) on NP69 cells following 24 h exposure.

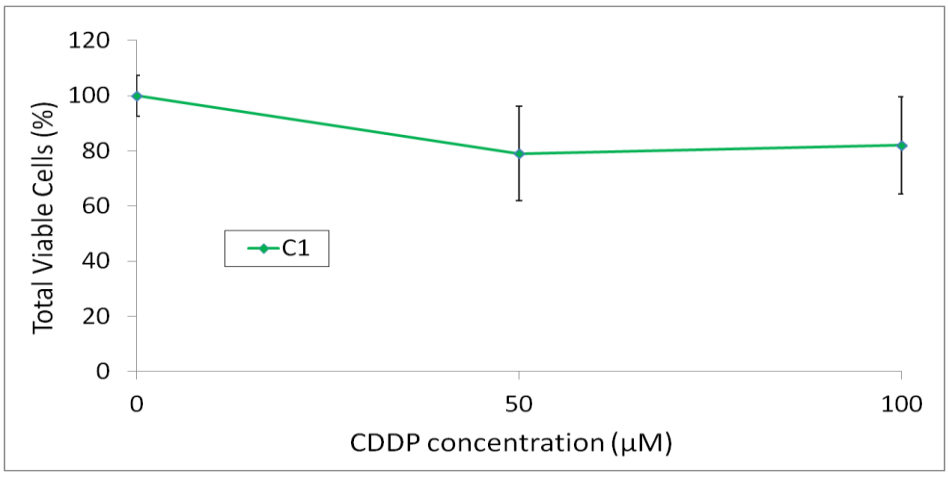

Figure 4.6: Comparative dose-response curve for ACA in combination with CDDP on NP69 cells following 24 h exposure.

† Simultaneous treatment with ACA at constant concentration of 3.0 µM and 0 - 100.0 µM of CDDP for 24 h

4.3.2 Cytotoxic effects of DMSO on various cell lines

DMSO is a widely used solvent for hydrophobic compounds although it has been shown to be cytotoxic at high concentration (Da Violante *et al*., 2002). As DMSO was used to dissolve both ACA and CDDP in this study, its effects at various concentrations on the various cell lines used were evaluated to ensure that the cytotoxicity observed was induced by ACA and/or CDDP, and not DMSO.

Figure 4.7 showed that both NP69 and Ca Ski cells were not significantly affected by the cytotoxic effects of DMSO, since the total of viable cells for both cell lines was maintained at around 90% even at the highest concentration of DMSO used. This showed that DMSO caused minimal reduction in cell viability and the cytotoxic effects observed were induced by ACA and/or CDDP.

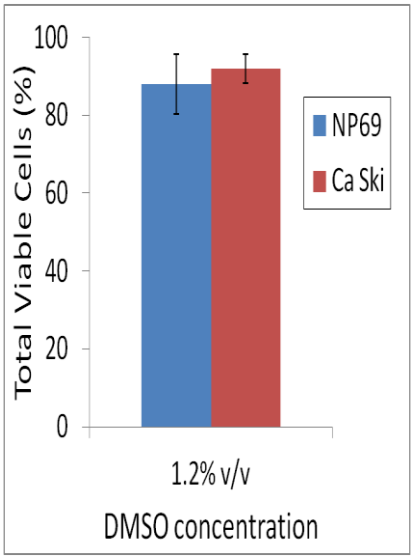

Figure 4.7: Cytotoxic effects of DMSO at 1.2% (v/v) on Ca Ski and NP69 cells following 24 h exposure.

4.4 RNA quality control

The quality of all extracted RNA samples was evaluated using UV spectrophotometry to determine its purity and Agilent RNA 6000 Nano Kit to determine its integrity before proceeding with the downstream experiments.

Results of all samples obtained from UV spectrophotometry and Agilent RNA 6000 Nano Kit are summarized in Table 4.4 and 4.5, respectively. To ensure the minimal presence of contaminants and inhibitors which might interfere with subsequent experiments, the ratio of A_{260nm}/A_{280nm} and A_{260nm}/A_{230nm} for all samples was maintained at above 1.8 with A_{320nm} of 0. RIN value for all samples was maintained at above 7.0 to ensure that only intact RNA was used for downstream experiments.

Table 4.4: RNA analysis using UV spectrophotometry.

Sample name[†]	**A_{260nm}/A_{280nm}**	**A_{260nm}/A_{230nm}**	**A_{320nm}**
U1	2.09	2.29	0.00
U2	2.02	2.26	0.00
U3	2.04	2.18	0.00
A1	2.09	2.14	0.00
A2	1.98	3.14	0.00
A3	2.16	3.22	0.00
C1	2.12	2.03	0.00
C2	2.09	2.24	0.00
C3	2.06	2.16	0.00
AC1	2.02	2.16	0.00
AC2	2.15	1.96	0.00
AC3	2.04	2.24	0.00

[†] U denotes untreated cells; A denotes cells treated with standalone ACA; C denotes cells treated with standalone CDDP; AC: denotes cells treated with ACA in combination with CDDP; while number 1, 2 and 3 denotes biological replicates.

Table 4.5: RNA analysis using Agilent RNA 6000 Nano Kit.

Sample name†	RIN value	28S/18S ratio
U1	8.9	1.8
U2	8.0	1.6
U3	7.7	1.6
A1	8.5	1.6
A2	7.8	1.7
A3	8.6	1.8
C1	9.0	2.3
C2	8.7	2.0
C3	8.3	1.7
AC1	8.6	2.1
AC2	8.9	2.2
AC3	8.3	1.8

† U denotes untreated cells; A denotes cells treated with standalone ACA; C denotes cells treated with standalone CDDP; AC: denotes cells treated with ACA in combination with CDDP; while number 1, 2 and 3 denotes biological replicates.

4.5 MiRNA expression on Ca Ski cells

4.5.1 MiRNA microarray

To evaluate the effects of ACA and/or CDDP on miRNA expression, miRNA microarray was used to determine the global miRNA expression profiles following administration of ACA and/or CDDP. A total of 25 miRNAs were found to be significantly differentially expressed in response to ACA and/or CDDP, whereby 15 miRNAs were up-regulated while 10 miRNAs were down-regulated relative to untreated controls. Pattern of miRNA expression between different treatment regimes were markedly different, with the exception of hsa-miR-212 and hsa-miR-210 which showed similar increasing expression patterns in both ACA- and CDDP-treated Ca Ski cells and CDDP- and ACA in combination with CDDP-treated Ca Ski cells, respectively (Table 4.6).

Table 4.6: List of miRNA expression fold-change alterations following the administration of ACA and/or CDDP on Ca Ski cells over 2 h.

miRNA	miRBase Accession Number	Fold-change[†]	*p* value [‡]
Treatment: Standalone ACA			
hsa-miR-629	MIMAT0004810	2.55 ± 1.12	0.010
hsa-miR-212	MIMAT0000269	1.63 ± 0.45	0.039
hsa-miR-487a	MIMAT0002178	1.60 ± 0.41	0.018
hsa-miR-483-3p	MIMAT0002173	1.56 ± 0.41	0.026
hsa-miR-342-3p	MIMAT0000753	1.55 ± 0.22	0.004
hsa-miR-376a	MIMAT0000729	1.52 ± 0.13	0.015
hsa-miR-1262	MIMAT0005914	-1.53 ± 0.10	0.004
hsa-miR-875-3p	MIMAT0004923	-1.60 ± 0.13	0.007
hsa-miR-517[*]	MIMAT0002851	-1.69 ± 0.12	0.032
hsa-miR-411	MIMAT0003329	-1.99 ± 0.22	0.031
Treatment: Standalone CDDP			
hsa-miR-210	MIMAT0000267	2.41 ± 1.32	0.047
hsa-miR-1244	MIMAT0005896	2.34 ± 1.32	0.024
hsa-miR-663	MIMAT0003326	2.14 ± 0.91	0.040
hsa-miR-720	MIMAT0005954	2.07 ± 0.92	0.036
hsa-miR-513c	MIMAT0005789	1.77 ± 0.65	0.024
hsa-miR-212	MIMAT0000269	1.65 ± 0.52	0.032
hsa-miR-134	MIMAT0000447	-1.66 ± 0.14	0.047
hsa-miR-337-3p	MIMAT0000754	-1.85 ± 0.11	0.031
hsa-miR-130b	MIMAT0000691	-3.40 ± 0.21	0.040
Treatment: ACA in combination with CDDP			
hsa-miR-138	MIMAT0000430	2.13 ± 1.09	0.049
hsa-miR-744	MIMAT0004945	2.11 ± 1.15	0.045
hsa-miR-210	MIMAT0000267	2.02 ± 0.83	0.033
hsa-miR-523	MIMAT0002840	1.68 ± 0.44	0.044
hsa-miR-922	MIMAT0004972	1.67 ± 0.55	0.026
hsa-miR-1271	MIMAT0005796	-1.80 ± 0.06	0.002
hsa-miR-224	MIMAT0000281	-1.81 ± 0.20	0.048
hsa-miR-21[*]	MIMAT0004494	-1.87 ± 0.20	0.046

[†] Positive values denote up-regulation while negative values denote down-regulation as compared to untreated controls; [‡] p values ≤ 0.05 were considered significant.

4.5.2 Validation by qRT-PCR

A total of four candidate miRNAs (hsa-miR-138, hsa-miR-210, hsa-miR-224 and hsa-miR-744) were selected for validation by qRT-PCR using TaqMan® MicroRNA Assays (Applied Biosystems, USA) to confirm the findings of miRNA

microarray. These candidate miRNAs were selected as they exhibited the highest fold-change in combination chemotherapy involving ACA and CDDP. The hsa-miR-224 was selected over hsa-miR-21 for validation because it is lesser known compared to hsa-miR-21, which has a wide array of data available. Hence, further studies can be conducted on hsa-miR-224 in the future. Since hsa-miR-210 was identified as one of the differentially expressed miRNA in treatment involving CDDP, its result was also validated as well.

The U6 small nuclear RNA was used as an internal control to normalize RNA input. The fold-change was calculated using the $2^{-\Delta\Delta Ct}$ method (as described previously by Livak and Schmittgen, 2001) and presented as fold-expression changes relative to untreated controls after normalization with the internal control. Figure 4.8 showed a similar expression between miRNA microarray data and qRT-PCR data.

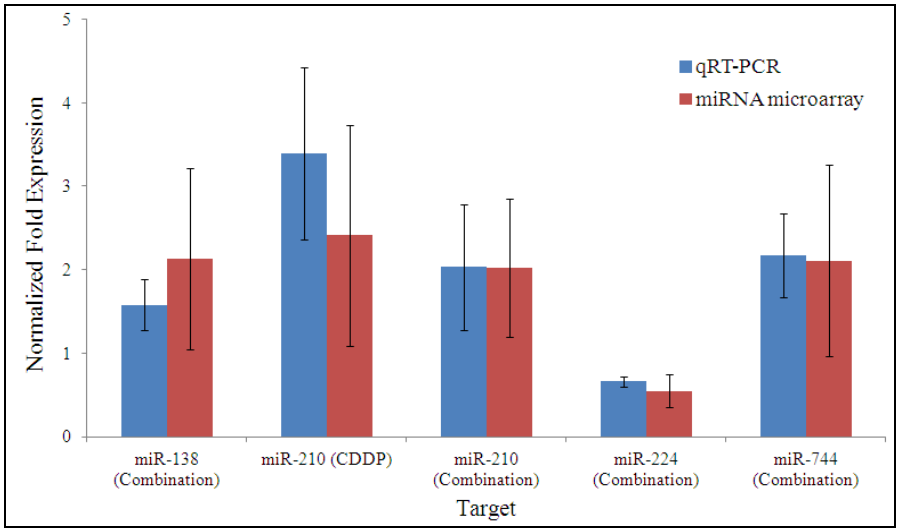

Figure 4.8: Normalized fold expression for hsa-miR-138, hsa-miR-210, hsa-miR-224 and hsa-miR-744.

† The qRT-PCR data were presented as fold-expression changes relative to untreated controls after normalization with U6 small nuclear RNA as internal control, while the miRNA microarray data were presented as fold-expression changes relative to untreated controls after normalization using Robust Multichip Average (RMA).

4.5.3 Correlation between miRNA microarray data and qRT-PCR data

Pearson correlation coefficient was used to determine the association between miRNA microarray data and qRT-PCR data. Result showed a correlation coefficient value, *r* of 0.842, with r^2 of 0.709, indicating a highly positive correlation between both sets of data (as depicted in Figure 4.9).

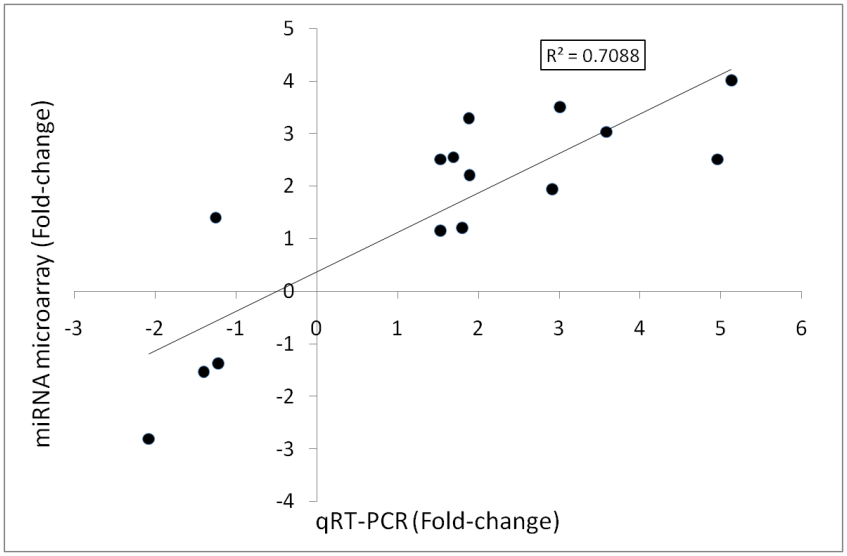

Figure 4.9: Correlation between miRNA microarray data and qRT-PCR data.

4.6 Bioinformatic analyses of miRNA gene targets

As hsa-miR-138, hsa-miR-210 and hsa-miR-744 exhibited the highest fold-change in combination chemotherapy, they were selected for bioinformatic analyses to determine their interaction with their putative gene targets. The putative gene targets of these candidate miRNAs were predicted using TargetScanHuman v5.2 and predicted target genes with total context score < 0 were then selected for gene-annotation enrichment analysis using DAVID v6.7 for tumorigenesis and cancer-related pathways. Key signaling pathways involved include wingless-type MMTV integration site family (WNT) pathway, nuclear factor kappa B (NF-κB) pathway, extracellular signal-regulated protein kinase (ERK) pathway, intrinsic pathway, transforming growth factor-beta (TGF-β) pathway, hypoxia pathway and calcium (Ca^{2+}) pathway. Since miRNAs

are negative gene regulators, these highlighted gene targets are thought to be down-regulated by these up-regulated miRNAs.

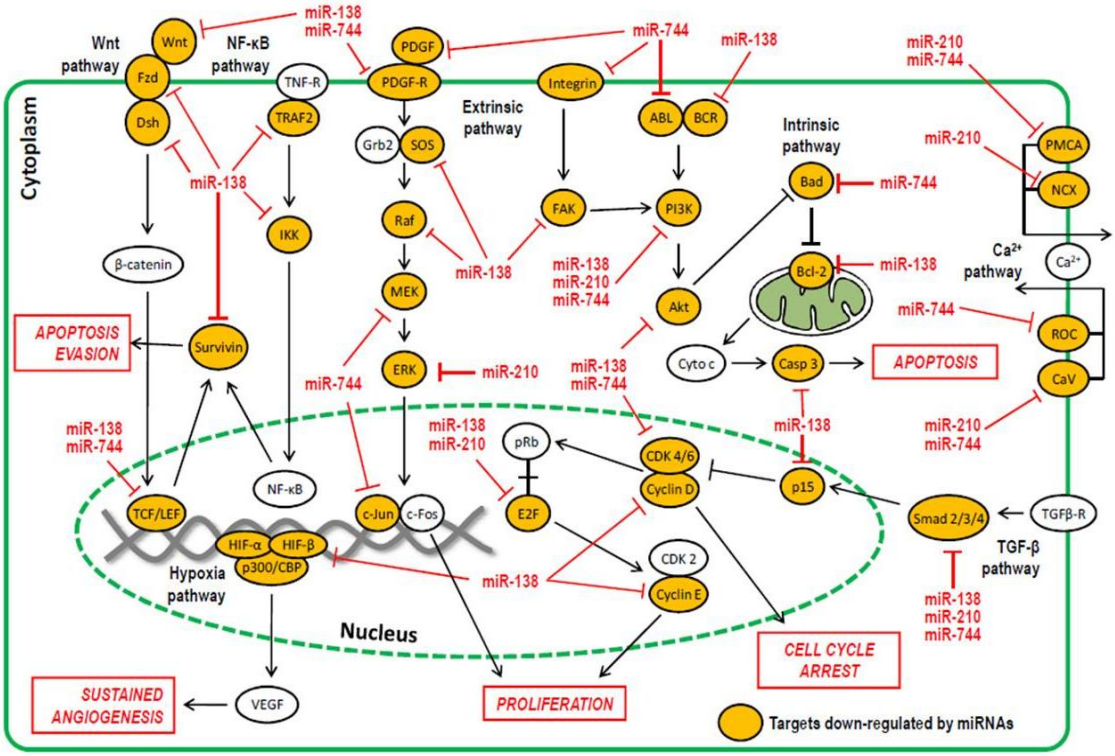

Figure 4.10: Pathway model comprising of interaction between candidate miRNAs with their putative target genes.

† Negative interactions were denoted as flat arrow heads, while positive interactions were denoted as closed arrow heads. Orange coloured symbols denote down-regulated targets, while clear coloured symbols denote targets unaffected by miRNAs.

CHAPTER 5: DISCUSSION

5.1 Cytotoxic effects of ACA and/or CDDP

Chemotherapy is the primary treatment in cervical cancer, with single agent CDDP being the current standard employed. Although treatment using CDDP results in high initial responsiveness, treatment failures due to toxicity and acquired resistance remains a major clinical problem. Thus, combination therapies are often favored over mono-targeted therapies to overcome these limitations. To date, topotecan and CDDP combination is the only regimen which demonstrated an improved overall survival, progression-free survival and response rate without diminishing life quality in patients in comparison to single agent CDDP (Cadron *et al*., 2007; Tao *et al*., 2008). This combination was approved for use in treatment of recurrent or persistent cervical cancer by the U. S. Food and Drug Administration in 2006. Hence, there is an on-going effort to identify not only new drug combinations, but also other therapy strategies including using miRNAs as biomarkers or targets to ameliorate chemotherapy in cervical cancer.

In this study, the cytotoxic effects of ACA and/or CDDP were first assessed using MTT cell viability assay which measures the mitochondrial dehydrogenase activity in viable cells. Results showed that both ACA and CDDP induced dose- and time-dependent cytotoxicity on Ca Ski cells when used as a standalone agent. This is both convenient and desirable as it allows for manipulation of the drugs' dosage and exposure period. This is because although low-dose, long-duration treatment is often preferred in chemotherapy to reduce the level of toxicities, a high-dose, short-duration treatment might be more beneficial in certain cases according to the Norton-Simon hypothesis, which states that chemotherapy results in a rate of regression in tumor volume that is proportional to the rate of growth for an untreated tumor of the same size

(Norton and Simon, 1986). Hence, a high-dose, short-duration treatment might result in higher cell kill over a period of time compared to a low-dose, long-duration treatment by preventing tumor recovery between treatments and development of drug resistance.

More importantly, synergistic effects were observed when cells were treated with ACA and CDDP simultaneously as well as sequentially over 24 h. These are important findings in many ways, as the synergistic interactions between ACA and CDDP could result in increased apoptosis and cell cycle arrest, reduced effective dose, decreased side-effects and lower recurrence of drug resistance. The synergistic effects observed suggest that ACA potentiates the cytotoxic effects in CDDP and may be explained, at least in part, by mechanisms of action in ACA. Earlier studies on ACA found rapid decrease in intracellular levels of glutathione (GSH) following administration of ACA (Higashida *et al*., 2009) and increased GSH is known to cause CDDP resistance through CDDP inactivation, enhanced DNA repair and reduced CDDP-induced oxidative stress (Siddik, 2003). Furthermore, studies have also showed that ACA inhibits activation of NF-κB and NF-κB-regulated gene expression such as cyclin D, c-Myc, survivin, inhibitors of apoptosis (IAPs), B-cell lymphoma 2 (Bcl-2), B-cell lymphoma-extra large (Bcl-xL), Bcl-2-related protein A1 (Bfl-1/A1) and FLICE-like inhibitory protein (FLIP) (Ichikawa *et al*., 2005). Thus, inhibition of these proliferative and anti-apoptotic gene products together with decrease in GSH intracellular levels would theoretically, augment efficacy of CDDP. The shift towards antagonistic effects in sequential 12 h pre-treatment with CDDP followed by ACA for 24 h corroborates with this notion, indicating that the chemosensitizing effect of Ca Ski cells by CDDP was absent in comparison to ACA. The resulting antagonistic effects could be because CDDP induced transcription of genes that counteract those induced by

ACA, or by blocking the transcription of genes induced by ACA when cells were pre-treated with CDDP.

5.2 Alterations in miRNAs expression patterns by ACA and/or CDDP

The main purpose of this study was to identify the different miRNAs involved in modulating response towards ACA and/or CDDP, and it was hypothesized that different treatment regimen would exhibit different miRNA expression pattern due to different mechanisms of action in ACA and CDDP. The miRNA microarray results showed that 10 miRNAs (6 up-regulated and 4 down-regulated); 9 miRNAs (6 up-regulated and 3 down-regulated); and 8 miRNAs (5 up-regulated and 3 down-regulated) were differentially expressed when cells were treated with standalone ACA; standalone CDDP; and ACA in combination with CDDP, respectively. Among the up-regulated miRNAs, hsa-miR-629, hsa-miR-210 and hsa-miR-138 exhibited the highest fold-change with a fold-change value of 2.41 ± 1.32, 2.41 ± 1.32 and 2.13 ± 1.09 in treatment involving standalone ACA, standalone CDDP and ACA in combination with CDDP, respectively. On the other hand, hsa-miR-411, hsa-miR-130b and hsa-miR-21* exhibited the highest fold-change among the down-regulated miRNAs in cells treated with standalone ACA, standalone CDDP, and ACA in combination with CDDP, with a fold-change value of -1.99 ± 0.22, -3.40 ± 0.21 and -1.87 ± 0.20, respectively.

Of these miRNAs, several of them have been previously associated with response towards anti-cancer drugs. For example, miR-212 over-expression induced sensitivity towards cetuximab in head and lung squamous cell carcinoma (Hatakeyama *et al.*, 2010) while down-regulation of miR-342 was associated with tamoxifen resistance in breast cancer cell lines (Cittelly *et al.*, 2010). It was also reported that silencing of miR-130b promotes multidrug resistance whereas its over-expression

increases sensitivity to CDDP and taxol in ovarian cancer (Yang *et al*., 2011). In a study conducted by Guo *et al*. in 2010, on small cell lung cancer, they found that sensitivity to anti-cancer drugs cisplatin, etoposide and doxorubicin greatly increased or reduced following transfection with miR-134 mimics or antagomirs, respectively. Another study showed that up-regulation of miR-138 increased sensitivity to CDDP and apoptosis in non-small cell lung cancer cells (Wang *et al*., 2010). Since miRNA microarray data from this study showed a directional correspondence to these earlier studies, this indicates that these miRNAs could also play a role in modulating response towards ACA and/or CDDP.

Besides that, it was also showed that the miRNA expression patterns between different treatment regimens are markedly different, with the exception of hsa-miR-210 and hsa-miR-212, with both miRNAs showing a similar increasing expression pattern between different treatments. The fold-change for hsa-miR-210 was found to be 2.41 ± 1.32 and 2.02 ± 0.83, when cells are treated with standalone CDDP and ACA in combination with CDDP, respectively while hsa-miR-210 exhibited a fold-change of 1.63 ± 0.45 in treatment involving standalone ACA, and 1.65 ± 0.52 in treatment involving standalone CDDP. This suggests that specific miRNAs are modulated in response towards ACA and/or CDDP and these differences in miRNA expression patterns in different treatment regimens could probably be due to the different spectrum of activity in ACA and CDDP. Thus, miRNAs expressions can be manipulated for future therapeutic advantages in cervical cancer drug combination treatment options.

Although microarrays conveniently allow for large-scale comparative expression profiles between samples to be analyzed, its data is inherently noisy and often yielded false positive and false negative results. In addition, there is also lack of agreement

between different microarray technologies. For these reasons, it is a common practice for microarray results to be validated with other technologies prior to publication or downstream experiments (Firestein and Pisetsky, 2002). Hence, in this study, four significantly differentially expressed miRNAs which exhibited the highest fold-change in combination chemotherapy were selected for validation by qRT-PCR, the current gold-standard method in data validation. Results from qRT-PCR indicates a highly positive correlation between miRNA microarray and qRT-PCR data with a correlation coefficient value, r of 0.842 and r^2 of 0.709.

5.3 Interaction between candidate miRNAs with their putative target genes

Since earlier results from this study had shown that ACA is able to potentiate cytotoxic effects of CDDP through synergistic interactions when used in combination, miRNAs found to be differentially expressed in treatment involving ACA in combination with CDDP were selected for bioinformatic analyses to evaluate the roles of these miRNAs in regulating genes involved in response towards ACA and CDDP. Three promising miRNA candidates (hsa-miR-138, hsa-miR-210 and hsa-miR-744), whose expression profiles were among those validated by qRT-PCR, were selected as they exhibited the highest fold-change. The putative gene targets of these candidate miRNAs were predicted using TargetScanHuman v5.2 and predicted target genes with total context score < 0 were then selected for gene-annotation enrichment analysis using DAVID v6.7 for tumorigenesis and cancer-related pathways. Key signaling pathways involved include wingless-type MMTV integration site family (WNT) pathway, nuclear factor kappa B (NF-κB) pathway, extracellular signal-regulated protein kinase (ERK) pathway, intrinsic pathway, transforming growth factor-beta (TGF-β) pathway, hypoxia pathway and calcium (Ca^{2+}) pathway. As miRNAs regulate gene expression negatively, these gene targets are thought to be down-regulated by the up-regulated miRNAs.

The ERK signaling cascade, a prominent component of the mitogen-activated protein kinase (MAPK) family, is one the pathways being targeted in the extrinsic pathway by these miRNAs. ERK is known to be involved in regulating cell proliferation and differentiation (Robinson and Cobb, 1997) and its activation has been associated with cervical cancer previously (Branca *et al*., 2004). The ERK cascade is initiated by growth factor binding to receptor tyrosine kinases and this leads to activation of the GTP-binding protein Ras, followed by serine kinase Raf (Avruch *et al*., 1994). Raf then activates MAPK kinase (MEK), a threonine/tyrosine dual specificity kinase that directly activates ERK (Crews *et al*., 1992). It was reported previously that activation of the ERK signaling pathway confers survival signals which counteract pro-apoptotic signals activated by c-Jun N-terminal kinases (JNK) and p38 signaling pathway, the other two subfamilies in MAPK (Xia *et al*., 1995). It was also shown that although CDDP activates ERK signaling and provides cells partial protection against CDDP, inhibition of this cascade actually enhanced CDDP cytotoxicity (Persons *et al*., 1999; Hayakawa *et al*., 1999). Since several members of the ERK signaling cascade are targeted for down-regulation by these miRNAs such as platelet-derived growth factor (PDGF), platelet-derived growth factor receptor (PDGFR), son of sevenless (Sos), Raf, MEK and ERK, inactivation of this pathway may lead to increased apoptosis and decreased cell proliferation.

The other pathway affected by these miRNAs is the TGF-β signaling pathway, which is involved in embryonic development, regulation of cell growth, differentiation and apoptosis (Massagué, 1998; Whitman, 1998; Derynck *et al*., 2001) and mutations or disruptions in its pathway have been linked to carcinogenesis (de Caestecker *et al*., 2000). TGF-β mediates cell cycle arrest by activating Smad2 or Smad3 to form a

complex with Smad4 to induce the expression of p15INK4B (Feng *et al*., 2000). This p15INK4B would then bind to and inactivate cyclin D-CDK4/6 complex and arrest cell cycle at G_1 phase (Reynisdóttir *et al*., 1995). Although p15INK4B, Smad3 and Smad4 were identified as among the putative targets, cyclin D, cylin E, CDK6 and E2F were also identified as possible targets at the same time. This indicates that cell cycle arrest at G_1 phase would occur regardless of p15INK4B expression if any of these (cyclin D, cylin E, CDK6 and E2F) is confirmed to be a true target.

Besides these, several members of the Wnt pathway are also affected such as Wnt ligand, Frizzled (Fzd) receptor, dishevelled (Dsh) phosphoprotein and lymphoid enhancer factor-T cell factor (LEF/TCF) transcription factors. In this canonical Wnt signaling pathway, the Fzd receptors transduce Wnt signals through Dsh phosphoprotein to stabilize β-catenin. The stabilized β-catenin then accumulates in cytoplasm and enters the nucleus to act as transcriptional coactivator of LEF/TCF (Rao and Kühl, 2010). Among known target genes regulated are proliferative genes such as cyclin D (Tetsu and McCormick, 1999) and c-Myc (He *et al*., 1998) as well as anti-apoptotic genes such as survivin (Kim *et al*., 2003). Hence, abrogation of this pathway via down-regulation of their members by miRNAs can result in cell cycle arrest and increase in apoptosis. Furthermore, these observations also suggest that treatment with ACA in combination with CDDP would lead to cell cycle arrest at G_0/G_1 phase, which has been shown to be consistent with previous studies on ACA's cell cycle arresting effects in oral cancer cell lines (Khalijah *et al*., 2010).

As both ACA and CDDP have been associated with apoptosis previously, it was not surprising to find anti-apoptotic proteins such as Bcl-2 and survivin among those down-regulated by these miRNAs. Another target predicted is Bcl-2-agonist death

promoter (Bad), a pro-apoptotic Bcl-2 family member which plays a dual role in apoptosis. De-phosphorylated Bad has pro-apoptotic effects as it can form heterodimer with Bcl-xL and Bcl-2 and allow for apoptosis to occur (Yang *et al*., 1995), while Bad phosphorylation by Akt has anti-apoptotic effects because it will then interact with the 14-3-3 protein, resulting in its sequestration in cytoplasm and renders it unable to bind with Bcl-xL or Bcl-2 and inhibit apoptosis (Zha *et al*., 1996). Surprisingly, caspase-3 was also identified as one of the putative gene targets since it is an executioner caspase which plays an important role in triggering a caspase cascade that eventually leads to apoptosis. Although it is contradictory and caspase-3 is only a putative target of these miRNAs, this needs to be validated experimentally. It should be noted that apoptosis could still occur via a caspase-3 independent apoptotic pathway in the absence of caspase-3, as previously associated with CDDP-induced cell death (Henkels and Turchi, 1999). Alternatively, studies have also shown that apoptosis can still be activated by caspase-7 in absence of caspase-3, albeit less effectively (Twiddy *et al*., 2006). It should also be noted that DNA laddering, a hallmark of apoptosis, following treatment with ACA on Ca Ski cells has been reported previously (Khalijah *et al*., 2010).

Furthermore, tumor necrosis factor receptor-associated factor 2 (TRAF2) and IκB kinase (IKK), which are involved in NF-κB activation, was also found among the predicted targets. Upon activation by tumor necrosis factor-alpha (TNF-α), tumor-necrosis factor receptor (TNFR) interact with tumor necrosis factor receptor type 1-associated death domain (TRADD) and TRAF2 to activate IKK, which then targets inhibitor of NF-κB (IκB) for degradation, leading to NF-κB activation (Dixit and Mak, 2002). NF-κB activation has been associated with CDDP resistance previously and consistent with this, NF-κB inhibitors have been reported to augment CDDP activity in cancer cells (Venkatraman *et al*., 2005). This NF-κB inactivation may be mediated by

ACA, as it was previously reported that ACA inactivates NF-κB through IKK (Ichikawa *et al*., 2005).

Other than these pathways, calcium channels involved in regulating intracellular level of Ca^{2+} such as plasma membrane Ca^{2+} ATPase (PMCA), sodium-calcium exchanger (NCX), receptor-operated calcium channels (ROC) and voltage-gated calcium channels (CaV) were also identified among the putative targets. The intracellular calcium levels play an important role in regulating various processes ranging from secretion to movement, proliferation and cell death. There is also wide experimental evidence supporting the notion that prolonged and unregulated elevations in intracellular calcium level can lead to cell death via apoptosis or necrosis (Berridge *et al*., 2000). Moreover, studies have also shown that CDDP induced elevation in the levels of intracellular calcium and this elevation is associated with increased apoptotic death (Kawaii *et al*., 2006; Splettstoesser *et al*., 2007; Florea and Büsselberg, 2009). Hence, any perturbation in the intracellular calcium level would affect apoptosis in the cells.

These miRNAs also affect hypoxia signaling pathway by targeting CREB-binding protein (CBP) and hypoxia-inducible factors (HIFs) such as HIF-α and HIF-β. Studies showed that hypoxia induced CDDP resistance and this resistance can be reversed by silencing HIF-1α, a major transcription factor that plays a central role in hypoxia response (Song *et al*., 2006). Hence, down-regulation of this gene by the miRNAs would enhance the effects of CDDP. Other putative targets identified and whose expressions have been associated with cisplatin resistance are focal adhesion kinase (FAK) (Chen *et al*., 2008), c-Jun (Pan et al., 2002) as well as PI3K and AKT (Lee *et al*., 2005). As these genes are also targeted by the miRNAs, down-regulation of

these targets by miRNAs might increase sensitivity towards CDDP and subsequently result in increase of apoptosis and cell cycle arrest, consistent with data obtained from MTT cell viability assays which showed synergistic effects when ACA is combined with CDDP.

5.4 Future research

In the current study, it was demonstrated that ACA and CDDP induced cytotoxicity on Ca Ski cells in dose- and time-dependent manner when used as standalone agents. It was also shown that ACA is able to potentiate the cytotoxic effects of CDDP through synergistic interactions when used in combination. Furthermore, miRNAs modulated in response towards ACA and/or CDDP were also identified. The gene targets of selected miRNA candidates were also predicted and depicted in a hypothetical pathway model consisting of interaction between candidate miRNAs with their putative gene targets.

Hence, for future research, the predicted targets for the miRNAs should first be confirmed experimentally using luciferase reporter assay, based on the proposed pathway model elucidated in this study. Following that, the roles of miRNAs in modulating response towards anti-cancer drugs can then be evaluated by transfecting the cells with miRNA precursor molecules to identify the gain-of-function phenotypes and/or miRNA inhibitors to identify the loss-of-function phenotypes, to look into its corresponding effects, i.e. anti-proliferative and/or apoptotic effects.

CHAPTER 6: CONCLUSION

The main aims of this study were to investigate the combined effects of a natural compound 1'S-1'-acetoxychavicol acetate (ACA) with cisplatin (CDDP) on human cervical carcinoma cells Ca Ski, and to identify microRNAs (miRNAs) modulated in response towards ACA and/or CDDP. Results from the *in vitro* studies demonstrated that ACA and CDDP induced dose- and time-dependent cytotoxicity when used as standalone agents. Furthermore, it was also shown that ACA is able to potentiate the cytotoxic effects of CDDP when used in combination through synergistic interactions. It was also found that specific miRNAs are dysregulated in response to both standalones and combination chemotherapy, providing important insights that miRNAs expression is affected by treatment regimen or mechanism of action in the anti-cancer drugs. The hypothetical pathway model comprising of interaction between candidate miRNAs with their putative target genes indicated that the cytotoxic effects induced from treatment with ACA in combination with CDDP might be regulated by miRNAs expression. To date, this study describes for the first time, the linkage between miRNA expression profiles in response to both standalones and combination chemotherapy. This is also the first time that ACA was shown to be able to potentiate the cyototoxic effects of CDDP through synergistic interactions. Therefore, this study provides a platform to methodically study the roles of these miRNAs in modulating response towards anti-cancer drugs. A better understanding in the interactions between miRNAs with their specific gene targets can help us to delineate the molecular mechanism underlying anti-cancer drug response and provide potential therapeutic approaches by exploiting the miRNA expression to improve efficacies in combination chemotherapy.